AD-310 002

364100

NAVAL PROVING GROUND

DAHLGREN, VIRGINIA

REPORT NO 4-46

BALLISTIC SUMMARY - PART II
THE SCALE EFFECT AND THE OGIVE EFFECT

1 April 1946

NPG 4-46 P II

[redacted]

NOTICE OF CHANGE IN CLASSIFICATION
OPNAV 5511-11 (4-66) S/N 0107-786-1000

ORIGINATOR OR HIGHER DISCIPLINARY HAVING CONTROL OVER SUBJECT MATTER

COMMANDER, NAVAL SURFACE WEAPONS CENTER
DAHLGREN, VIRGINIA 22448

DATE

25 July 1977

ADDRESSEES OF ORIGINAL DISTRIBUTION (Use Standard Navy Distribution List numbers if applicable. Additional sheets may be attached if more space is necessary.)

DX 21

The material described below has been changed in classification as indicated. Addressees shall change the classification of copies held.

☐ CHANGED TO _____ ☐ DOWNGRADED TO _____ ☒ DECLASSIFIED

DATE AND DESCRIPTION OF MATERIAL (Avoid identification which would cause this form to be classified.)

PG Report 446, April 1946, "Ballistic Summary--Pt. 2, The Scale Effect and the Ogive
ffect".
EMARK WITH DISTRIBUTION STATEMENT "A" - Approved for Public Release
Distribution Unlimited.

SIGNATURE OF AUTHORIZING OFFICIAL

G. W. PHILBRICK, Security Officer

NAVAL PROVING GROUND
DAHLGREN, VIRGINIA

Captain David I. Hedrick, USN*
Commanding Officer

Captain K. M. McLaren, USN
Ordnance Officer

NPG Report No. 4-46

BALLISTIC SUMMARY - PART II
THE SCALE EFFECT AND THE OGIVE EFFECT

A. V. HERSHEY
Lieutenant, USNR

APPROVED FOR PUBLIC RELEASE,
DISTRIBUTION UNLIMITED.

1 April 1946

NPG Report No. 4-46

BALLISTIC SUMMARY - PART II
THE SCALE EFFECT AND THE OGIVE EFFECT

1. For some years the Naval Proving Ground has been assiduously engaged in the study of the penetration of armor by projectiles. Pursuance of this work to conclusive results must be predicated upon well substantiated theories defining the performances of the materials involved under the various possible conditions.

2. Particularly necessary in the more immediately practical field of armor study and evaluation is the need for dependable plate penetration charts or tables. In 1943 Lieut. A. V. Hershey, USNR was assigned the task of preparing such charts. In prosecution of the assigned task he conducted an exhaustive study, employed for the first time new methods of attack and developed new theories concerning the phenomena incident to the penetration of plates by projectiles.

3. During the latter years of World War II, Lieut. Hershey prepared a series of nine reports which are being published by the Naval Proving Ground under titles as follows:

(1) ANALYTICAL SUMMARY. PART I. THE PHYSICAL PROPERTIES OF STS UNDER TRIAXIAL STRESS.

Object: To summarize the available data on the physical properties of Class B Armor and STS under triaxial stress.

(2) ANALYTICAL SUMMARY. PART II. ELASTIC AND PLASTIC UNDULATIONS IN ARMOR PLATE.

Object: To analyse the propagation of undulations in armor plate; to summarize previous analytical work and to add new analytical work where required in order to complete the theory for ballistic applications.

(3) ANALYTICAL SUMMARY. PART III. PLASTIC FLOW IN ARMOR PLATE.

Object: To analyse the plastic flow in armor plate adjacent to the point of impact by a projectile.

(4) ANALYTICAL SUMMARY. PART IV. THE THEORY OF ARMOR PENETRATION.

Object: To summarize the theory of armor penetration in its present state of development, and to develop theoretical functions which can be used as a guide in the interpretation of ballistic data.

(5) BALLISTIC SUMMARY. PART I. THE DEPENDENCE OF LIMIT VELOCITY ON PLATE THICKNESS AND OBLIQUITY AT LOW OBLIQUITY.

Object: To compare the results of ballistic test with the prediction of existing formulae, and with the results of theoretical analysis; to find the mathematical functions which best represent the fundamental relationship between limit velocity, plate thickness, and obliquity at low obliquity.

(6) BALLISTIC SUMMARY. PART II. THE SCALE EFFECT AND THE OGIVE EFFECT.

Object: To determine the effect of scale on ballistic performance, and to correlate the projectile nose shape with the results of ballistic test.

(7) BALLISTIC SUMMARY. PART III. THE WINDSHIELD EFFECT, AND THE OBLIQUITY EFFECT FOR COMMON PROJECTILES.

Object: To analyse the action of a windshield during impact, and to develop mathematical functions which best represent the ballistic performance of common projectiles.

(8) BALLISTIC SUMMARY. PART IV. THE CAP EFFECT, AND THE OBLIQUITY EFFECT FOR AP PROJECTILES.

Object: To determine the action of a cap during impact, and to develop mathematical functions which best represent the ballistic performance of AP projectiles.

(9) BALLISTIC SUMMARY. PART V. THE CONSTRUCTION OF PLATE PENETRATION CHARTS OR TABLES.

Object: To summarize the results of analysis in the form of standard charts or tables.

4. The opinions and statements contained in these reports are the expressions of the author, and do not necessarily represent the official views of the Naval Proving Ground.

David I. Hedrick

DAVID I. HEDRICK
Captain, USN
Commanding Officer

PREFACE

AUTHORIZATION

The material in this report has been basic to the construction of plate penetration charts. It was authorized by BuOrd letter NP9/A9 (Re3) dated 9 January 1943.

OBJECT

To determine the effect of scale on ballistic performance, and to correlate the projectile nose shape with the results of ballistic test.

SUMMARY

Limit velocities for perforation at different scales, but with geometrically similar combinations of plate and projectile, vary logarithmically with the dimensions of the plates or projectiles. The scale effect may be correlated with the effect of strain rate on stress in the armor steel.

A change in nose shape from one projectile design to another has an effect on the depth to which the projectiles penetrate into homogeneous plate at striking velocities less than limit, and modifies also the limit velocity for perforation. If a series of projectiles be arranged in the order of depth of penetration, they appear also in the correct order of limit velocity.

The ellipsoid, the ogive, the cone, and the cylinder are all special cases of a two-parameter family of surfaces. The nose shapes of service projectiles may also be represented to within a few hundredths of a caliber by members of this same family. Corresponding to each projectile nose shape there exists an ellipsoidal nose shape which would have the same ballistic properties as the actual nose shape. In the correlation of ballistic performance, the two parameters of the general family of nose shapes may be reduced to a single parameter, the ratio of major axis to minor axis for the equivalent ellipsoid. Values for the parameters have been computed for the projectiles of interest to the service.

TABLE OF CONTENTS

		Page
I	INTRODUCTION	1
II	THE BALLISTIC PARAMETERS	3
III	STATISTICAL ANALYSIS OF BALLISTIC DATA	7
IV	THE SCALE EFFECT	10
V	THE OGIVE EFFECT	11
VI	BALLISTIC DATA	18
VII	REFERENCES	30

LIST OF FIGURES

Figure (1) NPG Photo No. 2976 (APL). The Plate Penetration Coefficient for 0° Obliquity.

Figure (2) NPG Photo No. 3027 (APL). The Obliquity Function θ.

Figure (3) NPG Photo No. 3028 (APL). Cylindrical polar coordinates of a point on a projectile nose contour.

Figure (4) NPG Photo No. 3029 (APL). Parameters of the Ogive.

Figure (5) NPG Photo No. 3030 (APL). 2 pdr and 3" AP M79 projectile nose contours.

Figure (6) NPG Photo No. 3031 (APL). Frankford Arsenal experimental Dw. 52, Dw. 53 and Dw. 54 projectile nose contours.

Figure (7) NPG Photo No. 3032 (APL). Frankford Arsenal experimental Dw. 55, Dw. 56, and Dw. 57 projectile nose contours.

Figure (8) NPG Photo No. 3033 (APL). Frankford Arsenal experimental Dw. 58 and Dw. 59 projectile nose contours.

Figure (9) NPG Photo No. 3034 (APL). 3" Experimental flat nosed and conical nosed projectile contours.

Figure (10) NPG Photo No. 3035 (APL). 4" Comm Mk. 16-1, 5" Comm Mk 38-1 and 5" Comm Mk 46-2 projectile nose contours.

Figure (11) NPG Photo No. 3036 (APL). 6" Comm Mk. 27-7, 8" Comm Mk.17-2, and 8" AP Mk 11-1 projectile nose contours.

Figure (12) NPG Photo No. 3037 (APL). 20mm AP C-20mm-1, 37mm AP M51B2, and 3" AP M61 projectile nose contours.

Figure (13) NPG Photo No. 3038 (APL). 3" AP Type A, 3" AP Type A-1, and 3" AP Mk 29-2 projectile nose contours.

Figure (14) NPG Photo No. 3039 (APL). 8" AP Mk 19-1, 8" AP Mk 19-4, and 8" AP Mk 21-3 projectile nose contours.

Figure (15) NPG Photo No. 3040 (APL). 6" AP Mk 35-5, 12" AP Mk 18-1, and 16" AP Mk 8-6 projectile nose contours.

Figure (16) NPG Photo No. 3041 (APL). 14" AP Mk 16-2, 14" AP Mk 16-4, and 14" AP Mk 16-8 projectile nose contours.

Figure (17) NPG Photo No. 3042 (APL). The variation of stress with strain rate.

Figure (18) NPG Photo No. 3043 (APL). The scale effect.

Figure (19) NPG Photo No. 3044 (APL). The depth of penetration.

Figure (20) NPG Photo No. 3045 (APL). The effect of nose shape on the depth of penetration.

Figure (21) NPG Photo No. 3046 (APL). The ogive effect at $\epsilon/d < .5$.

Figure (22) NPG Photo No. 3047 (APL). The ogive effect at $\epsilon/d > .5$.

LIST OF TABLES

Table I — NPG Photo Nos 3025 (APL) and 3026 (APL). Projectile Data.

Table II — Parameters of the ogive.

Table III — Plate penetration coefficients for cal. .60 monobloc projectiles vs. homogeneous plate of 115000 (lb)/(in)^2 tensile strength.

Table IV — Plate penetration coefficients for geometrically similar scale model 2 pdr projectiles, vs homogeneous plate of 115000 (lb)/(in)^2 tensile strength.

Table V — Plate penetration coefficients for 2 pdr. projectiles with tangent ogives of various calibers radius, vs. homogeneous plate of 115000 (lb)/(in)^2 tensile strength.

Table VI — Plate penetration coefficients for uncapped 37mm AP M51B2 projectiles, 3" AP M79 projectiles, and other 3" monobloc projectiles vs Class B armor and STS of 115000 (lb)/(in)^2 tensile strength.

Table VII — Plate penetration coefficients for AP bombs vs Class B armor of 115000 (lb)/(in)^2 tensile strength at 15°C.

I INTRODUCTION

It was assumed for many years by the U. S. Navy that all projectile designs are equivalent in ballistic performance as long as they are undeformed. This assumption was fully justified before the modern AP projectile development program, because there were in reality only minor variations in projectile design. The projectiles of recent interest have varied, however, from cal. 30 small arms ammunition at one extreme to flat nosed major caliber bombs at the other, and differences in projectile design can no longer be ignored in any accurate analysis.

A few of the variables which enter into the analysis of armor penetration are the mass of the projectile, the diameter of the projectile, the thickness of the plate, the shape of the projectile nose contour and the ductility of the plate material. The conditions of impact are defined by the obliquity and the striking velocity. The results of impact in an incomplete penetration are summarized by the depth of penetration, which is measured from the tip of the projectile, at the instant of maximum travel, to a reference plane which is tangent to the plate just outside of the coronet but inside of the dish. The results of impact in a complete penetration are summarized by the remaining velocity. From the results of impact may be derived the limit velocity, or that striking velocity which would just put the major portion of the projectile completely through the plate with zero remaining velocity.

The individual values of depth of penetration and limit velocity for each impact vary capriciously from impact to impact partly because of fluctuations in plate quality. The average values of depth of penetration and limit velocity vary continuously however with the dimensions and shape of the projectile.

The limit velocities for non-deforming monobloc projectiles, with geometrically similar combinations of plate and projectile, decrease on the average with increase in the dimensions of the plates or projectiles. The decrease in limit velocity with increase in scale is partly the result of a simultaneous decrease in static tensile strength. As the plate thickness is increased, the difficulty of control during manufacture increases, and the thick plates are usually heat treated to a low hardness in order to avoid brittle failure on impact. The limit velocity for a ductile plate is primarily a function of the dynamic tensile strength and a plate may have several limit velocities, even for the same static tensile strength, if the microstructure is varied. The existence of a true scale

effect would only be revealed by a series of ballistic tests with geometrically similar monobloc projectiles fired against geometrically similar pieces sliced from the same thick plate. Such tests would require a difficult machining operation.

An approximate estimate of the scale effect may be derived, nevertheless, from existing ballistic data for nondeforming projectiles all with nearly the same nose shape but tested against different plates. Corrections may be applied to the data for small variations in nose shape, but measurements of the actual dynamic tensile strengths are not available. Corrections for variations in tensile strength must therefore be based on the assumption that the relationship between dynamic tensile strength and static tensile strength follows the general trend for steels of constant microstructure. Corrections[4] for tensile strength should be applied only in part to data for plates whose hardness is near the critical hardness for brittle failure, and should probably be omitted altogether from comparisons between Class B armor and STS. Thus, specimens of Class B armor have been found by the group at the California Institute of Technology to have nearly the same dynamic tensile strengths as specimens of STS, even though the static tensile strengths varied from 98000 (lb)/(in)^2 for the Class B armor to 116000 (lb)/(in)^2 for the STS.

The limit velocity for non-deforming pointed projectiles decreases on the average as the sharpness of the point is increased and plate failure in each impact occurs with the formation of a star crack. The limit velocity for non-deforming round nosed projectiles, on the other hand, decreases on the average as the nose contour approaches a flat cylinder, and plate failure in each impact usually occurs with the formation of a punching or plug. The existence of an ogive effect is revealed by a series of ballistic tests with monobloc projectiles of various nose shapes all fired against the same plate. The number of such tests which have been completed is sufficient to outline the general trends of the ogive effect.

Details of these ballistic data, which best illustrate the scale effect and the ogive effect have been released in previous reports, references (1) to (3) but are summarized in Tables III to VII in the present report.

A semiquantitative theory of armor penetration has been completed for the 3" AP M79 projectile, and details of the theory will be released in later reports. The results of the theory are used in the

present report to interpret the results of test. The 3" AP M79 projectile is the most extensively investigated monobloc projectile, and has therefore been used as the reference standard for comparisons.

II THE BALLISTIC PARAMETERS

The results of ballistic test may conveniently be summarized in terms of a number of ballistic parameters. The impact parameter F_S, the plate penetration coefficient $F(e/d,\theta)$, and the residual velocity function F_R may all be defined in terms of the projectile mass m, the projectile diameter d, the plate thickness e, the obliquity θ, the striking velocity v_S, the limit velocity v_L, and the remaining velocity v_R by the equations

$$F_S = \frac{m^{\frac{1}{2}} v_S \cos\theta}{e^{\frac{1}{2}} d}$$

$$F(e/d,\theta) = \frac{m^{\frac{1}{2}} v_L \cos\theta}{e^{\frac{1}{2}} d}$$

$$F_R = \frac{m^{\frac{1}{2}} v_R \cos\theta}{e^{\frac{1}{2}} d}$$

These parameters are convenient to use in the representation of ballistic data, since they are directly proportional to velocity, and do not vary rapidly with plate thickness or obliquity.

Of more fundamental significance are the impact energy parameter U_S, the limit energy function $U(e/d,\theta)$, and the residual energy function U_R, which are defined in terms of F_S, $F(e/d,\theta)$ and F_R

by the equations

$$U_S = \left(\frac{e}{d}\right)F_S^2$$

$$U(e/d,\theta) = \left(\frac{e}{d}\right)F^2(e/d,\theta) = \frac{mv_L^2\cos^2\theta}{d^3}$$

$$U_R = \left(\frac{e}{d}\right)F_R^2$$

These parameters are proportional to the kinetic energy of the projectile at normal obliquity.

Ballistic performance may be interpreted with equal validity in terms of either of the functions $F(e/d,\theta)$ or $U(e/d,\theta)$. The projectile mass in the functions is expressed in (lb), the projectile diameter is expressed in (ft), the plate thickness in (ft), and the limit velocity in (ft)/(sec).

The scale effect for a given projectile is best represented by the ratio $1+\sigma$ between the limit energy function for the given projectile and the limit energy function for a 3" projectile of the same geometrical shape. The ogive effect is similarly represented by the ratio $1+\omega$ between the limit energy function for the given projectile and the limit energy function for a projectile of the same caliber but with the nose contour of the 3" AP M79 projectile. The ratio between the limit energy function for any projectile and the limit energy function for the 3" AP M79 projectile is then equal to the product $(1+\sigma)(1+\omega)$.

The limit energy function for the standard projectile at low obliquity is given[4] by the equation

$$U(e/d,\theta) = \left(\frac{e}{d}\right)\Phi^2\theta\cos\theta$$

in which Φ is a function of e/d and θ is a function of θ. The functions Φ and θ are expressed graphically by Figures (1) and (2).

The shape of any projectile nose contour is defined analytically by a relationship between the cylindrical polar coordinates r and s of a point on the surface of the projectile. The distance r is measured from the axis of the projectile, and the distance s is measured from a plane perpendicular to the axis, through the tip of the nose. The coordinates r, s are illustrated in Figure (3). The dimensions of the nose contour are the radius a of the bourrelet, and the length b of the nose from bourrelet to tip.

The ellipsoid, the ogive, and the cone are special cases of a two-parameter family of surfaces, whose general equation is

$$\frac{s}{a} = \frac{b}{a}\left(1 - \sqrt{1 - \alpha\frac{r}{a} - (1-\alpha)\frac{r^2}{a^2}}\right)$$

The two parameters in the equation are b/a and α.

The equation for an ellipsoid is

$$\frac{s}{a} = \frac{b}{a}\left(1 - \sqrt{1 - \frac{r^2}{a^2}}\right)$$

for which the value of α is zero. The ratio b/a is the ratio between the major axis and the minor axis of the ellipsoid.

The equation for an ogive* is

$$\frac{s}{a} = \frac{b}{a}\left(1 - \sqrt{1 - \left(1 - \frac{a^2}{b^2}\right)\frac{r}{a} - \frac{a^2r^2}{b^2a^2}}\right) \qquad (1)$$

*According to the strictest definition, the ogive is a surface of revolution described by the arc of a single circle which is tangent to the bourrelet.

The parameters b/a and α for an ogive are given in terms of the radius R of the arc by the equations

$$\frac{b}{a} = \frac{1}{a}\sqrt{R^2 - (R-a)^2} = \sqrt{2\frac{R}{a} - 1}$$

and

$$\alpha = 1 - \frac{a^2}{b^2} = \frac{\frac{R}{a} - 1}{\frac{R}{a} - \frac{1}{2}}$$

The equation for the cone is

$$\frac{z}{a} = \frac{b}{a}\left(\frac{r}{a}\right)$$

for which the value of α is equal to + 2. The ratio b/a is the ratio between the altitude of the cone and the radius of the base.

The flat nose or cylinder is obtained from the general equation, for any value of α, by setting b/a equal to zero.

The nose contours of service type projectiles may also be represented to within a few hundredths of a caliber by members of the same family. Values of the parameters b/a and α have been chosen for all of the projectiles of ballistic interest. The parameters have been so chosen that the volume contained between the projectile nose contour and a circumscribed cylinder is the same for the approximate contour as for the actual contour. The volume of the circumscribed cylinder is $\pi a^2 b$, while the volume contained in the space between the projectile nose contour and the circumscribed cylinder is given by the integral

$$2\pi \int_0^a z\,dr$$

The ratio between the two volumes is given for the approximate contour in terms of α by the equation

$$\frac{2\pi\int_0^{\alpha} zrdr}{\pi a^2 b} = \frac{\frac{3}{4}\alpha^2 - \frac{4}{3}\alpha + \frac{1}{8}}{(1-\alpha)^2} + \frac{\frac{1}{8}\alpha(2-\alpha)^2}{(1-\alpha)^{\frac{5}{2}}}\cos^{-1}\frac{\alpha}{2-\alpha} \qquad (2)$$

Values of this ratio have been computed for a series of values of α and are listed in Table II. The ratio between the two volumes is found for the actual contour by numerical integration.

The values of b/a and α for service type projectiles were found by a process of successive approximations. From trial values of b/a and α were calculated points on a trial contour, which was then compared graphically with the actual contour. The parameters were readjusted until the distance between the two contours was reduced to a minimum. The final values for b/a and α are listed in Table I and are plotted in Figure (4). The final trial contours for a few of the projectiles, are compared with the actual contours in Figures (5) to (16), where the trial contours are represented by dotted lines and the actual contours are represented by solid lines.

III STATISTICAL ANALYSIS OF THE BALLISTIC DATA

Separation of the scale effect and the ogive effect from the effects of variations in plate quality requires a statistical analysis of the ballistic data.

If the impact energy parameter U_S in any impact happens to be less than the limit energy function $U(e/d, \theta)$, the impact is an incomplete penetration, but if the impact energy parameter U_S happens to be more than the limit energy function $U(e/d, \theta)$, the impact is a complete penetration. The ballistic data at major caliber scale usually consist of two impacts on each plate, whose values of U_S bracket the value of $U(e/d, \theta)$. The actual bracket may usually be replaced by a narrower estimated bracket, which is based on the depth of penetration and the remaining velocity of the projectile. The brackets vary in width from plate to plate, and the wide brackets deserve less statistical weight than the narrow brackets.

If the limit energy function $U(e/d, \theta)$ fluctuates from plate to plate in accordance with the normal law of errors, then the frequency of occurrence of an individual deviation β from the true mean u for all plates is given by the expression

$$\frac{h}{\sqrt{\pi}} e^{-h^2\beta^2}$$

in which h is the precision constant of the fluctuation.

If a pair of impacts at two different values of U_S were repeated an unlimited number of times on different plates, each time with the same two values of U_S, then the value of $U(e/d, \theta)$ would fall between the two values of U_S with a frequency equal to

$$\frac{1}{\sqrt{\pi}} \int_{h\epsilon^*}^{h\epsilon^0} e^{-\beta^2} d\beta$$

in which ϵ^* is the deviation of the smaller value of U_S from the mean value of $U(e/d, \theta)$, and ϵ^0 is the deviation of the larger value of U_S.

The collected ballistic data consist of a group of brackets, each with a different pair of values for U_S. If a group of n pairs of impacts were repeated an unlimited number of times, each time with the same set of values for U_S, then the limit energy function would fall between the two values of U_S on every pair of impacts in the group with a frequency N which is given by the product

$$N = \Pi \left(\frac{1}{\sqrt{\pi}} \int_{h\epsilon_k^*}^{h\epsilon_k^0} e^{-\beta^2} d\beta \right)$$

in which ϵ_k^* and ϵ_k^0 are the deviations of the two values of U_S in the k^{th} pair of impacts. A particular group of limit determinations would occur with the greatest frequency in that series of plates for which N is a maximum with respect to variations in u and h. The most likely values

of u and h are therefore those which satisfy the conditions

$$-\frac{1}{hN}\left(\frac{\partial N}{\partial u}\right) = \Sigma \frac{e^{-h^2\epsilon_k^{o2}} - e^{-h^2\epsilon_k^{*2}}}{\int_{h\epsilon_k^*}^{h\epsilon_k^o} e^{-\beta^2}d\beta} = 0$$

$$+\frac{h}{N}\left(\frac{\partial N}{\partial h}\right) = \Sigma \frac{h\epsilon_k^o e^{-h^2\epsilon_k^{o2}} - h\epsilon_k^* e^{-h^2\epsilon_k^{*2}}}{\int_{h\epsilon_k^*}^{h\epsilon_k^o} e^{-\beta^2}d\beta} = 0$$

If ϵ_k^* is nearly equal to ϵ_k^o, these equations are simplified to the equations

$$-\frac{1}{hN}\left(\frac{\partial N}{\partial u}\right) = -2\Sigma h\epsilon_k e^{-\frac{1}{8}h^2(\epsilon_k^o-\epsilon_k^*)^2} = 0$$

$$+\frac{h}{N}\left(\frac{\partial N}{\partial h}\right) = \Sigma e^{-\frac{1}{8}h^2(\epsilon_k^o-\epsilon_k^*)^2} - 2\Sigma h^2\epsilon_k^2 e^{-\frac{1}{8}(\epsilon_k^o-\epsilon_k^*)^2} = 0$$

in which ϵ_k is the average of ϵ_k^* and ϵ_k^o. In the limit with ϵ_k^* equal to ϵ_k^o, the equations are further simplified to the conventional equations of least squares

$$-\frac{1}{hN}\left(\frac{\partial N}{\partial u}\right) = -2\Sigma h\epsilon_k = 0$$

$$+\frac{h}{N}\left(\frac{\partial N}{\partial h}\right) = n - 2\Sigma h^2\epsilon_k^2 = 0$$

The values of u and h for a particular group of data are found from the above equations of maximum likelihood by successive approximations.

The standard deviation of an individual value of $U(e/d,\theta)$ from the mean value u is given in terms of the precision constant h by the expression

$$\frac{1}{\sqrt{2}h}$$

IV THE SCALE EFFECT

The instantaneous velocities of all projectiles, at any particular stage of penetration, are almost, though not quite, the same for geometrically similar combinations of plate and projectile. The duration of any stage of penetration varies therefore almost inversely with the dimensions of the plate or projectiles. The distributions of strain in the armor around the noses of all projectiles, at the given stage of penetration, are geometrically similar. The strain rates for all projectiles at the given stage of penetration, also vary, therefore, almost inversely with the dimensions of the system. The stress in the armor may be represented as a logarithmic function of strain rate in the range of strain rates which occur during projectile impact. Direct measurements of the variation of stress with strain rate for several steels are plotted in Figure (17). The stress in STS increases approximately 4% per unit increase in the natural logarithm of strain rate, in the range of strain rates greater than 200 $(sec)^{-1}$.

The function which was therefore chosen in 1944 by the Naval Proving Ground to represent the relationship between the scale effect σ and the projectile diameter d is given by the equation

$$\sigma = - (.04 \pm .02)\log(4d) \qquad (3)$$

Equation (3) is basic to NPG Sk 650. It is represented in Figure (18) by Curve I.

The nearest approach to a scale model of a 3" AP M79 projectile in STS is represented by the data in Table III for the cal .60 Expr. Dw 51 projectile in Plate No. N-1. The cal .60 projectile has the same ogive as the 3" projectile, but differs in the type of carrier. (The cal .60 projectile has a base cup, whereas the 3" projectile has a rotating band.) Plate No. N-1 was a nickel-chromium alloy plate of standard STS composi-

tion with 0.27% carbon. The data for Plate No. N-1 give a value of σ which agrees accurately with the predictions of Equation (3). Plate No. H-4, on the other hand, was a chromium molybdenum alloy plate with 0.50% carbon, and the data for Plate No. H-4 give a larger value of σ.

Values of σ have been derived from the various groups of data in Tables III to VII, simultaneously with values of ω. The average values of σ are plotted for comparison in Figure (18), both with and without correction to a standard static tensile strength of 115000 $(lb)/(in)^2$. Each uncorrected average value is bracketed in the figure by a pair of open symbols whose distance apart is twice the standard deviation of the mean value. The data indicate the existence of a real scale effect, of the magnitude predicted by theory.

A statistical analysis has been made of the data in Table VII for AP bombs. The ratio $(1+\sigma)(1+\omega)$, between the limit energy function for the AP bombs and the limit energy function for the 3" AP M79 projectile, is tabulated in the ninth column of the table. The statistical weight to be assigned to each ratio is listed in the tenth column. The ratio fluctuates about a weighted mean of .924 with a standard deviation of .08. The precision constant of the fluctuation is equal to 9. Some of the plates in this series may have had hardnesses above the critical hardness for brittle failure, and the mean value of the ratio $(1+\sigma)(1+\omega)$ is probably therefore too small.

V THE OGIVE EFFECT

Data on the depth of penetration p of projectiles into Class B armor and STS have been collected during routine ballistic tests. The average data may be represented by curves which express the ratio p/d as a function of the ratio v_S/v_L, with a separate curve for each value of e/d. A study of the data for all projectiles has indicated that, at striking velocities near limit, the penetration curves for two different projectile shapes are nearly parallel, and only differ from each other by a constant difference in p/d. The curves for one projectile shape may be obtained from the curves for a different shape by a vertical shift. A set of standard curves have been derived from all the data, and are plotted in Figure (19). There exists for each nose contour a correction g which, when added to the value of p/d taken from Figure (19), gives the correct mean value of p/d for the given contour. A value for g has been selected to represent each of the projectiles which have been adequately investigated, and the values of g are listed in Table I.

Values of the ogive effect ω have been derived from the various groups of data in Tables IV to VII, simultaneously with values of σ.

The two most thoroughly investigated monobloc projectiles which are listed in the tables are the uncapped 37mm AP M51B2 projectile and the 3" AP M79 projectile. The ratio $(1+\sigma)(1+\omega)$ between the limit energy function for the 37mm projectile and the limit energy function for the 3" projectile was found to have a mean value of 1.062 ± .01 in a range of e/a from .4 to 1.7. The corresponding value of ω is 0.033.

The values of g and ω depend on both the parameters b/a and α. Thus, the 8" AP Mk 19-1 projectile and the 8" AP Mk 19-4 projectile have nearly the same values of b/a, but entirely different values of g. Similarly the 3" Expr. Dw 53 projectile and the 3" Expr. Dw 55 projectile both have nearly equal values of ω which are distinctly not zero, yet the values of b/a for these two projectiles straddle the value of b/a for the 3" AP M79 projectile. If the points in a plot of α vs b/a such as Figure (4) be marked with the average values of g or ω for each projectile, then it is found that series of contours of equal ballistic performance may be drawn in the plot which are not inconsistent with the data collected to date. Each of the contours of equal ballistic performance crosses the axis $\alpha = 0$ at a value of b/a equal to the ratio of major axis to minor axis for that ellipsoid which would have the same ballistic properties as another projectile on the same contour. The ratio b^*/a of the major axis to the minor axis for the equivalent ellipsoid is expressed empirically in terms of the parameters b/a and α for the actual projectile, by the equation

$$\frac{b^*}{a} = \frac{\frac{b}{a}}{\sqrt{1 - 1.2\alpha + .6\alpha^2}} \qquad (4)$$

Values of b^*/a for various projectiles are listed in Table I, and one contour of equal ballistic performance has been plotted in Figure (4). The penetration parameter g and the ogive effect ω are plotted against b^*/a in Figures (20) to (22). Inspection of the figures shows that the ballistic performance varies consistently with b^*/a.

The ratio $1+\omega$, between the limit energy function for a pointed projectile and the limit energy function for the standard projectile, was found to decrease with increase in b^*/a, at a rate which varied with e/d. The rate of variation of $1+\omega$ with b^*/a at 0° obliquity was apparently zero at some value of e/d between .244 and .65, and increased with increase in e/d.

The ratio $1+\omega$, between the limit energy function for a blunt projectile and the limit energy function for the standard projectile, was found to decrease with decrease in b^*/a.

The properties of the ogive effect for a pointed projectile in a thick plate may be interpreted in terms of the plastic flow of the plate material adjacent to the point of impact. A disturbance in the interior of a solid medium is propagated by two waves which move with different velocities. The leading wave is a compressional or longitudinal wave, while the trailing wave is an equivoluminal or transverse wave. The velocity of propagation of the longitudinal wave is determined primarily by the bulk modulus, while the velocity of propagation of the transverse wave is determined by the rate of work hardening. A longitudinal wave originates at the surface of the Projectile, but both longitudinal waves and transverse waves are reflected wherever the longitudinal wave reaches a free surface. The velocity of propagation of a longitudinal wave is everywhere greater than the velocity of the projectile, whereas the velocity of propagation of a transverse wave is zero at a distance of approximately one tenth caliber from the surface of the impact hole, but increases with distance from the impact hole to a velocity greater than the velocity of the projectile. There is a zone next to the impact hole which is reached only by the longitudinal wave.

The plastic flow in this zone is nearly irrotational, but the transverse waves at a distance from the point of impact are able to maintain the plate material in a state of equilibrium. The plastic energy which would be required in the limiting case of pure irrotational flow, has been found by calculation to be greater than the energy which would be required in the limiting case of pure equilibrium flow, by an amount which is zero at an e/d of 0.5, but increases with increase in e/d. Approximately half of the plastic work on the medium in a plate of caliber thickness is actually performed under conditions of irrotational flow, and half is performed under conditions of equilibrium flow. An increase in the length of the projectile nose contour increases the duration of impact and increases the relative amount of equilibrium flow, with a consequent decrease in the amount of plastic work for perforation.

Ductile failure by shear occurs in the armor near the point of impact. The plate failure begins with the formation of a star crack near a pointed projectile, and a circular crack near a blunt projectile. The plastic energy required to open the petals of a star crack is spread out to a distance from the impact hole, whereas the energy required to punch out a cylindrical plug is concentrated along the cylindrical surface of the plug. The energy required by a pointed projectile is therefore greater than the energy required by a flat nosed projectile.

TABLE I

PROJECTILE DATA

Projectile	Mfg.	(lb) Mass	% Charge	% Cap	% WS	Cap Hardness	Drive a	Drive b/a	Drive b²/a	K
cal .30 AP M2	FA	0.0119	none							
cal .50 AP M2	FA	0.0580	none				0.61	4.2	6.0	0.76 ± 0.03
cal .50 AP E-5	PR	0.062	none	none	none		.80	2.24	3.44	
20 mm AP C-20mm-1	FA	.31	none	21.2	none	64 R_C	.20	1.91	2.16	
37 mm AP M51B2	FA	1.88	none	13.0		62 R_C	.10	2.5	2.66	
2 pdr AP	BR	2.4	none	none	none		.71	2.06	3.07	
3" Comm Mk 3-5	AF	13.0		none	none		.86	2.65	4.13	
3" Comm Mk 3-7	AF	13.0		none	none		.86	2.65	4.13	
3" AP Type A	CS	14.1	1.4	11.1	none	54 R_C	.10	1.92	2.04	0.10 ± 0.02
3" AP Type A-1	BS	14.1	1.4	11.3	none		.51	2.02	2.74	
3" AP Dw DA302-SC (Mk 11 cap)	BS	13.6		11.1	none		.51	2.02	2.74	
3" AP Dw DA302-HC (Mk 11 cap)	BS	13.6		11.1	none		.51	2.02	2.74	
3" AP Dw DA303 (Light cap)	BS	13.9		10.4	none		.51	2.02	2.74	
3" AP Dw DA304 (Heavy cap)	BS	14.65		16.1	none		.51	2.02	2.74	
3" AP Dw 3001 (6" AP Mk 11-1)	CS	14.5		5.2	none		.375	2.67	3.35	
3" AP Mk 29 (Dw DA305)	BS	13.0		16.1	2.6		.33	1.94	2.37	
3" AP Mk 29-1	CS	13.0		16.1	2.9		.33	1.94	2.37	
3" AP Mk 29-2	OLDS	13.0		16.1	3.0	58 R_C	.33	1.94	2.37	
3" AP Mk 29-A	CS	13.0		11.5	2.9		.33	1.96	2.37	
3" AP Mk 29-B	CS	13.0		15.4	2.9		.33	1.94	2.37	
3" AP Mk 29-C	CS	13.0		10.9	2.9		.33	1.94	2.37	
3" AP Mk 29-E23	OLDS	13.0		16.6	3.0		-0.05	1.70	1.65	
3" AP Mk 29-E34	OLDS	13.0		18.1	3.0		-0.11	1.86	1.275	
3" AP M61 (Dw DA301)	CS BS	14.6		14.3	2.3	47 R_C	+0.82	1.925	2.97	
3" AP M62	BS	14.8		13.9	2.3	53 R_C	.33	1.94	2.37	
3" AP M62	CHEV	14.8		13.9	2.3	58 R_C	.33	1.94	2.37	
3" AP M79	LT FA	15.0	none	none	none		0.824	2.30	3.68	0.47 ± 0.03
3" Expr Dw 52 (Hemisphere)	FA	15.2	none	none	none		.000	1.00	1.00	
3" Expr Dw 53 (Type A-1 body)	FA	15.2	none	none	none		.33	2.00	2.45	
3" Expr Dw 54 (Type A body)	FA	15.2	none	none	none		-0.09	1.92	1.32	
3" Expr Dw 55 (Type A-1 cap)	FA	15.3	none	none	none		+0.04	2.73	2.80	
3" Expr Dw 56 (M51B2 cap)	FA	15.3	none	none	none		-	-	-	
3" Expr Dw 57 (Mk 11 cap)	FA	15.0	none	none	none		-	-	-	
3" Expr Dw 58 (3 cal ogive)	FA	15.3	none	none	none		.909	3.32	5.22	
3" Expr Dw 59 (4 cal ogive)	FA	15.3	none	none	none		.934	3.88	6.11	
3" AP Expr (7.6 lb flat nose)	FA	7.4	none	none	none		-	.00	.00	
3" AP Expr (11 lb flat nose)	FA	10.7	none	none	none		-	.00	.00	
3" AP Expr (15 lb flat nose)	FA	14.9	none	none	none		-	.00	.00	
3" AP Expr (flat nose + WS)	CS	13.0	none	none	1.6		-	.00	.00	
4" Comm Mk 10-1	HP	33		none	none					
4" Comm Mk 16-1	BW	33	3.0	4.7	3.9		.80	2.80	3.84	
5" Comm Mk 15-14	JR	50		none	none					
5" Comm Mk 32-4	CS	54	4.8	none	8.0					
5" Comm Mk 38-1	CS	55	3.7	7.0	7.0	80 R_B	.87	2.70	4.34	
5" Comm Mk 46-1	CS	55	3.7	5.0	6.8		.94	2.53	3.11	
5" Comm Mk 46-2	BS	55	3.7	6.8	6.8		.94	2.53	3.11	
6" Comm Mk 20-2	MP	105		none	none					
6" Comm Mk 20-4	CS	105		none	none					
6" Comm Mk 27-1	BS	105	2.1	4.0	5.1		.79	2.25	3.44	0.41 ± 0.02
6" Comm Mk 27-2	CS	105	-	-	5.4		.86	2.61	4.07	
6" Comm Mk 27-3	MS	105	2.1	6.5	5.1		.70	2.325	3.45	
6" Comm Mk 27-4	MS	105	2.1	6.5	5.1		.70	2.325	3.45	0.43 ± 0.02
6" Comm Mk 27-5	CS	105	2.4	5.2	5.5		.86	2.61	4.07	
6" Comm Mk 27-6	MS	105	2.1	5.7	5.0		.70	2.325	3.45	
6" Comm Mk 27-7	CS	105	2.1	5.2	5.1		.86	2.61	4.07	0.59 ± 0.10
6" Comm Mk 27-8 (Dw DA607)	BS	105	2.1	4.0	5.1		.79	2.25	3.44	
6" Comm Mk 33-1	BS	105	2.1	5.2	5.1		.86	2.61	4.07	
6" Comm Mk 33-2	CS	105	2.1	5.2	5.1		.86	2.61	4.07	
155 mm SAP M112	BS	100	1.4	5.3	4.8					
6" AP Mk 9-1	FS	105		7.5	none		.47	2.90	3.80	
6" AP Mk 9-6	FS	105		9.1	-		.47	2.90	3.80	
6" AP Mk 35-1	CS	130	1.5	15.6	2.6		.21	1.77	2.01	
6" AP Mk 35-2	MS	130	1.5	10.0	2.5		.16	1.825	2.09	
6" AP Mk 35-3	BS	130	1.5	19.1	2.5		.21	1.77	2.01	
6" AP Mk 35-4 (Dw 3001)	BS	130	1.5	20.6	2.5		+0.14	1.61	1.73	
6" AP Mk 35-5	MS	130	1.5	20.0	2.5	53 R_C	-0.13	1.495	1.505	
6" AP Mk 35-6	CS	130	1.5	19.6	2.5		-0.07	1.515	1.45	
6" AP Mk 35-7	BS	130	1.5	20.6	2.5	53 R_C	+0.14	1.61	1.73	
152 mm AP Mk 1-1	MS	130	1.5	20.0	2.5		-0.13	1.495	1.505	

TABLE I
(Continued)

PROJECTILE DATA

Projectile	Mfg.	(Lb) Mass	% Explosive	% Cap	% WS	Cap Material	Ogive			g
							a	b/a	b'/a	
8" Comm Mk 14-1	BS	260	4.2	4.7	5.6		0.59	2.65	3.74	0.43 ± 0.03
8" Comm Mk 15-1	BS	260	4.4	10.9	8.0		.49	2.45	3.26	
8" Comm Mk 17-1	CS	260	4.0	--	5.6		.71	2.45	3.65	
8" Comm Mk 17-2	BS	260	4.0	4.7	5.7		.59	2.45	3.74	
8" Comm Mk 17-3	BS	260	4.0	5.9	5.5		.76	2.57	3.69	
8" Comm Mk 17-4	CS	260	4.0	4.1	5.7		.71	2.45	3.65	0.47 ± 0.04
8" Comm Mk 17-4 (Mod.)	CS	260	4.0	8.0	0.6					
8" AP Mk 7-9	BS	260	2.1	6.0	1.1		.375	2.69	3.38	
8" AP Mk 11-1	BS	260	2.1	5.5	1.3	225 BHN	.375	2.69	3.38	0.37 ± 0.02
8" AP Mk 19-1	CS	260	1.4	18.2	4.6		.71	1.88	2.77	0.31 ± 0.02
8" AP Mk 19-2	BS	260	1.4	18.5	4.5					
8" AP Mk 19-3	BS	260	1.4	16.5	5.1					
8" AP Mk 19-4	CS	260	1.4	16.7	9.3		.16	1.855	2.02	0.10 ± 0.03
8" AP Mk 19-5	BS	260	1.4	17.2	5.0		.16	1.855	2.02	
8" AP Mk 19-6	CS	260	1.4	16.7	5.3		.16	1.855	2.02	
8" AP Mk 20-1	BS	260	1.3	18.6	4.6					
8" AP Mk 20-2	BS	260	1.3	18.2	4.5					
8" AP Mk 20-4	BS	260	1.3	16.2	5.1					
8" AP Mk 20-5	BS	260	1.3	17.1	5.1					
8" AP Mk 21-1	CS	333	1.5	17.5	2.3	53 R_C	.12	1.735	1.885	
8" AP Mk 21-2	BS	335	1.5	17.0	1.4	53 R_C	.24	1.46	1.69	
8" AP Mk 21-3	CS	335	1.5	17.3	1.3	53 R_C	.12	1.735	1.865	
12" AP Mk 14-6	BS	675	2.6	5.7	1.1		.67	2.90	3.85	
12" AP Mk 15-6	-	670	2.6	6.2	0.6		.47	2.90	3.85	0.52 ± 0.04
12" AP Type A-1	BS	1140	1.5	13.0	1.2		.31	2.00	2.42	
12" AP Mk 18-1	CS	1140	1.5	10.9	1.2		.09	1.84	1.94	
14" AP Mk 16-2	BS	1500	1.5	8.5	2.1		.70	2.18	3.24	0.40 ± 0.04
14" AP Mk 16-3	BS	1500	1.5	8.5	2.1		.59	2.20	3.10	
14" AP Mk 16-4	BS	1500	1.5	10.0	2.0		.77	1.96	2.98	0.57 ± 0.02
14" AP Mk 16-7	BS	1500	1.5	10.1	2.1		.27	1.94	2.88	
14" AP Mk 16-8	CS	1500	1.5	10.2	2.3		.10	1.835	1.935	
14" AP Mk 16-9	BS	1500	1.5	11.8	2.4		+0.26	1.94	2.27	
14" AP Mk 16-10	BS	1500	1.5	12.2	2.3		-0.13	1.525	1.41	
14" AP Mk 20-1	CS	1500	1.5	10.1	2.4		+0.04	1.70	1.74	
16" AP Mk 2-1	BS	2100	2.4	5.5	1.1		.47	2.90	3.85	
16" AP Mk 5-4	BS	2240	1.5	10.6	2.2		.16	1.945	1.92	
16" AP Mk 6-1	CS	2700	1.5	9.7	1.8		.48	2.12	2.85	
16" AP Mk 6-2	BS	2700	1.5	7.6	1.7		.14	2.04	2.22	
16" AP Mk 6-3	BS	2700	1.5	11.0	1.8		.34	1.90	2.54	
16" AP Mk 6-4	CS	2700	1.5	9.8	1.8		.17	2.17	2.41	
16" AP Mk 6-5	BS	2700	1.5	9.3	1.7		.16	1.97	2.17	
16" AP Mk 6-6	BS	2700	1.5	11.6	1.2		.17	1.85	2.05	
16" AP Type B-1	CS	3850	1.5	10.0	1.7		.06	2.05	2.10	
1000 lb AP Bomb Mk 33		975	15.0	none	none		.91	2.51	3.04	
1600 lb AP Bomb Mk 1-1	CS	1540	15.0	none	none		.89	2.57	4.03	

Manufacturer

AP = American Cal and Foundry Co.
BS = Bethlehem Steel Co.
BR = British.
BC = Budd Wheel Co.
CHEV = Chevrolet Division, General Motors Corp.
CS = Crucible Steel Co.
FA = Frankford Arsenal
FS = Firth Sterling Steel Co.
HP = Harrisburg Pipe and Pipe Bending Co.
IR = Ingersoll Rand Co.
LT = The Letourneau Co.
MP = Machine Products Co.
MH = The Midvale Co.
OLDS = Oldsmobile Division, General Motors Corp.
PA = Picatinny Arsenal
PR = Princeton Range

$$\% \text{ Charge} = \frac{\text{Weight of Explosive}}{\text{Total Weight}} \times 100$$

$$\% \text{ Cap} = \frac{\text{Weight of Cap or Hood}}{\text{Total Weight}} \times 100$$

$$\% \text{ WS} = \frac{\text{Weight of Windshield}}{\text{Total Weight}} \times 100$$

a and b/a are parameters in the approximate equation for the nose contour, such that b/a is the ratio of length to semidiameter of the approximate nose contour, and $(1/2)a(b/a)$ is the cotangent of the semiangle at the tip of the nose.

b'/a is the ratio of major axis to minor axis of the equivalent ellipsoidal nose.

g is the increase, due to difference in nose shape, of the ratio p/d, where p is the depth of penetration at striking velocities less than limit, and d is the projectile diameter.

Table II

Parameters of the Ogive

R (Calibers)	$\frac{b}{a}$	α	$\frac{2\pi\int_0^a xr\,dr}{\pi a^2 b}$
.5	1.000	0	$\frac{1}{3}$
.6	1.183	.286	.3682
.8	1.483	.545	.4019
1.0	1.732	.666	.4184
1.2	1.949	.737	.4282
1.5	2.236	.800	.4371
2.0	2.646	.857	.4454
3.0	3.317	.909	.4530
4.0	3.873	.933	.4566
∞	∞	1.000	.4667

VI BALLISTIC DATA

Table III - Plate penetration coefficients for cal .60 monoblcc projectiles at normal obliquity vs homogeneous plate corrected for tensile strength to 115000 (lb)/(in)^2 tensile strength. (Reference (1))

Projectile Type	d	Plate No.	Brinell Hardness	$\frac{e}{d}$	Uncorrected $F(\frac{e}{d},\theta)$	Corrected $F(\frac{e}{d},\theta)$	$(10^{-6})U(\frac{e}{d},\theta)$	1+C	1+C
AP Dw 51	".588	N-1	248	1.45	54000	53000	40.7	1.067	
AP Dw 51	"	H-4	255	1.52	56100	54600	45.4	1.109	1.000
AP Dw 53	"	"	"	1.52	56500	54900	45.8		1.012
AP Dw 54	"	"	"	1.52	56200	54700	45.5		1.006
AP Dw 55	"	"	"	1.52	56800	55200	46.4		1.023
AP Dw 58	"	"	"	1.52	53800	52300	41.6		.918
AP Dw 59	"	"	"	1.52	53000	51500	40.3		.891

UNCLASSIFIED

Table IV - Plate penetration coefficients for geometrically similar scale model service type 2 pdr. projectiles at normal obliquity vs homogeneous plate corrected for tensile strength to 115000 (lb)/(in)^2 tensile strength. Ogival radius = 1.40 calibers. (Reference (2))

d	Plate No.	Brinell Hardness	$\frac{e}{d}$	Uncorrected $F(\frac{e}{d}, \theta)$	Corrected $F(\frac{e}{d}, \theta)$	$(10^{-9}) B(\frac{e}{d}, \theta)$	$(1+\sigma)(1+\omega)$
.1896	2970	259	.767	53300	51500	20.1	1.175
"	2975	250	.977	54400	53200	27.6	1.184
"	2976	267	1.418	55800	53400	40.4	1.083
"	2980	257	1.831	57600	55900	57.2	1.096
.1540	2973	250	.536	53700	52600	14.83	(1.33)
"	2976	267	.777	52400	50100	19.50	1.105
"	2980	257	1.004	54000	52300	27.5	1.137
"	2986	255	1.501	54900	53200	42.5	1.059
"	2994	269	2.055	59400	58700	66.1	1.082
.1990	2980	257	.548	51600	50000	13.70	(1.20)
"	2986	255	.819	51400	49800	20.3	1.081
"	2994	269	1.121	54400	51900	30.2	1.090
"	3003	265	1.610	55400	53200	45.6	1.035
"	3011	258	2.139	58500	56600	68.5	1.063
.1565	2994	269	.709	50000	47700	16.13	1.021
"	3003	265	1.019	51300	49300	24.8	1.008
"	3011	258	1.353	53900	52100	36.7	1.048
"	3011	259	2.013	55600	53700	58.0	.975

UNCLASSIFIED

Table V - Plate penetration coefficients for 2 pdr. projectiles with tangent ogives of various calibers radius, at normal obliquity vs homogeneous plate, corrected for tensile strength to 115000 (lb)/(in)^2 tensile strength. (Reference (2))

Ogival Radius	d	Plate No.	Brinell Hardness	$\frac{e}{d}$	Uncorrected $F(\frac{e}{d}, \theta)$	Corrected $F(\frac{e}{d}, \theta)$	$(10^{-8}) U(\frac{e}{d}, \theta)$	$(1+\sigma)(1+\omega)$
1.00	1".565	448	262	1.029	51000±1000	49200	24.9	1.000
1.40	"	"	"	1.029	50800±300	49000	24.7	.992
2.00	"	"	"	1.029	49800±200	48000	23.7	.952
1.00	1".565	1467	266	1.534	57500±400	55000	46.4	1.123
1.40	"	"	"	1.534	55200±100	53500	43.9	1.063
2.00	"	"	"	1.534	54000±200	51700	41.0	.992

Table VI - Plate penetration coefficients for uncapped 37mm AP M51B2 projectiles, 3" AP M79 projectiles, and other 3" monobloc projectiles vs Class B armor or STS corrected for tensile strength to 115000 (lb)/(in)^2 tensile strength. (Reference (3))

Projectile	Plate Number	Tensile Strength	θ	$\frac{t}{d}$	Uncorrected $F(\frac{t}{d}, \theta)$	Corrected $F(\frac{t}{d}, \theta)$	$(10^{-8})\theta(\frac{t}{d}, \theta)$	$(1+\sigma)(1+\omega)$
3" AP M79	1478	123000	30°	.655	43300±500		12.28	.998
3" AP Type A-cap	"	"	5.5°	.652	46500±500		14.10	.995
"	"	"	29.5°	.652	44000±1000		12.62	1.028
37mm AP M51B2-cap	8333*	98500	1°	.754	47400±500	49900	18.77	1.104
3" AP M79	9475	107000	.5°	1.68	51500±500	52600	46.5	1.000
3" Expr Dw 59 (4 cal. ogive)	"	"	.5°	1.69	46800±300	49800	41.9	.895
37mm AP M51B2-cap	40228	105000	1°	1.379	50400±300	52000	37.3	1.036
3" AP M79	"	"	30°	.669	40700±200	42000	11.80	.935
37mm AP M51B2-cap	40497	112000	.5°	1.007	50100±100	50500	25.7	1.060
3" AP M79	"	"	29.7°	.489	41200±200	41600	8.46	.995
37mm AP M51B1-cap	40500	120000	2°	1.005	50900±100	50200	25.3	1.047
3" AP M79	"	"	29.8°	.488	41000±200		8.20	.967
3" Expr (15 lb. flat nose)	"	"	1°	.488	28600±200		3.99	.405
"	"	"	30°	.488	30500±500		4.54	.535
"	"	"	45°	.496	32600±200		5.27	.567

* Section from the center of a 10.6" plate.

Table VI - (Continued)

Projectile	Plate Number	Tensile Strength	θ	$\frac{e}{d}$	Uncorrected $F(\frac{e}{d},\theta)$	Corrected $F(\frac{e}{d},\theta)$	$(10^{-6})\,U(\frac{e}{d},\theta)$	$(1+\sigma)(1+\omega)$
37mm AP M51B2-cap	40502	105000	1°	1.017	48800±500	50300	25.7	1.048
3" AP M79	"	"	.5°	.495	43900±100	45400	10.20	1.013
"	"	"	20°	.495	42100±100	43500	9.37	.995
"	"	"	30°	.490	40200±200	41700	8.52	1.000
3" AP M79	40819	117000	29.5°	.507	41300±200	41700	8.82	.986
3" Expr. (15 lb. flat nose)	"	"	30°	.507	31200±300	32100	5.22	.588
3" Expr. (15 lb. 150° cone)	"	"	31°	.510	33900±200	34900	6.21	.700
3" AP M79	40916	113000	29.5°	.498	41300±200	41700	8.66	.992
3" Expr. (15 lb. flat nose)	"	"	30°	.501	32000±200	32100	5.16	.589
"	"	87000	30°	.502	29300±200	32100	5.17	.589
37mm AP M51B2-cap	55909	118000	0°	.835	47900±300		19.16	.996
"	"	"	19.5°	.838	47600±300		19.00	1.048
"	"	"	30.3°	.841	44300±500		16.50	.997
3" AP M79	"	"	2°	.408	43500±500		7.72	1.008
3" AP Type A-cap	"	"	8°	.409	44000±1000		7.92	1.041
37mm AP M51B2-cap	56360	123000	3°	.433	40700±1000		7.17	.857
"	"	"	31°	.433	38500±500		6.42	.905
37mm AP M51B2-cap	60919	123000	2°	.443	47800±200		10.12	1.175
"	"	"	29.5°	.444	41800±500		7.75	1.041
3" AP Type A-cap	"	"	10°	.212	34000±500		2.45	1.028
"	"	"	31°	.213	30500±500		1.98	.957

Table VI - (Continued)

Projectile	Plate Number	Tensile Strength	θ	$\frac{e}{d}$	Uncorrected $F(\frac{e}{d}, \theta)$	Corrected $F(\frac{e}{d}, \theta)$	$(10^{-6}) / / (\frac{e}{d}, \theta)$	$(1+\sigma)(1+\omega)$
37mm AP M51B2-cap	83880	122000	4°	.504	48800±200		12.00	1.168
"	"	"	30.5°	.504	43300±500		9.45	1.076
3" AP M79	"	"	4°	.244	36900±200		3.32	1.051
3" Expr. Dw 52 (Hemisphere)	"	"	.5°	.244	34900±500		2.97	.940
3" Expr. Dw 53 (Type A-1 body)	"	"	2°	.244	36600±500		3.27	1.033
3" Expr. Dw 54 (Type A body)	"	"	1.5°	.244	35900±500		3.14	.994
3" Expr. Dw 55 (Type A-1 cap)	"	"	4°	.244	36900±200		3.32	1.053
3" Expr. Dw 56 (M51B2 cap)	"	"	0°	.244	35900±200		3.14	.994
3" Expr. Dw 57 (Mk 11 cap)	"	"	5°	.244	36200±300		3.20	1.015
3" Expr. Dw 58 (3 cal. ogive)	"	"	.5°	.244	37800±300		3.49	1.102
3" Expr. Dw 59 (4 cal. ogive)	"	"	1°	.244	37300±200		3.39	1.074
3" Expr. (11 lb. flat nose)	"	"	3°	.244	35500±500		3.08	.972
3" AP M79	"	"	45°	.244	31400±500		2.40	.939
3" Expr. Dw 52 (Hemisphere)	"	"	45°	.244	$\geq$ 35600		>3.09	>1.245
3" Expr. Dw 53 (Type A-1 body)	"	"	45°	.244	$\leq$ 33800		<2.79	<1.122
3" Expr. Dw 54 (Type A body)	"	"	45°	.244	$\geq$ 35300		>3.04	>1.224
3" Expr. Dw 55 (Type A-1 cap)	"	"	45°	.244	33500±200		2.74	1.103
3" Expr. Dw 56 (M51B2 cap)	"	"	45°	.244	31600±1000		2.44	.981
3" Expr. Dw 57 (Mk 11 cap)	"	"	45°	.244	31300±1000		2.39	.962
3" Expr. Dw 58 (3 cal. ogive)	"	"	45°	.244	30100±1000		2.21	.890
3" Expr. Dw 59 (4 cal. ogive)	"	"	45°	.244	30100±1000		2.21	.890
3" AP M79	87207	125000	0°	.809	44500±500		16.02	.866
"	"	"	30°	.809	43100±500		15.03	.946
3" AP Type A-cap	"	"	1°	.819	45000±500		16.58	.882
3" AP Type A-1-cap	"	"	28.5°	.819	45000±500		16.58	1.013
37mm AP M51B2-cap	87547	130000	3°	1.34	55500±1000	53100	37.8	1.082

Table VI - (Continued)

Tensile Strength	θ	$\frac{e}{d}$	Uncorrected $F(\frac{e}{d}, \theta)$	Corrected $F(\frac{e}{d}, \theta)$	$(10^{-8}) U(\frac{e}{d}, \theta)$	$(1+\sigma)(1+\omega)$
122000	4°	.504	48800±200		12.00	1.168
"	30.5°	.504	43300±500		9.45	1.076
"	4°	.244	36900±200		3.32	1.051
"	.5°	.244	34900±500		2.97	.940
"	2°	.244	36600±500		3.27	1.033
"	1.5°	.244	35900±500		3.14	.994
"	4°	.244	36900±200		3.32	1.053
"	0°	.244	35900±200		3.14	.994
"	5°	.244	36200±300		3.20	1.015
"	.5°	.244	37800±300		3.49	1.102
"	1°	.244	37300±200		3.39	1.074
"	3°	.244	35500±500		3.08	.972
"	45°	.244	31400±500		2.40	.969
"	45°	.244	$\geq$ 35600		>3.09	>1.245
"	45°	.244	$\leq$ 33800		<2.79	<1.122
"	45°	.244	$\geq$ 35300		>3.04	>1.224
"	45°	.244	33500±200		2.74	1.103
"	45°	.244	31600±1000		2.44	.981
"	45°	.244	31300±1000		2.39	.962
"	45°	.244	30100±1000		2.21	.890
"	45°	.244	30100±1000		2.21	.890
125000	0°	.809	44500±500		16.02	.866
"	30°	.809	43100±500		15.03	.946
"	1°	.819	45000±500		16.58	.882
"	28.5°	.819	45000±500		16.58	1.013
130000	3°	1.34	55500±1000	53100	37.8	1.089

Table VI - (Continued)

Tensile Strength	θ	$\frac{e}{d}$	Uncorrected $F(\frac{e}{d}, \theta)$	Corrected $F(\frac{e}{d}, \theta)$	$(10^{-a})U(\frac{e}{d}, \theta)$	$(1+\sigma)(1+\omega)$
130000	1°	.650	47300±200		14.54	1.026
"	4°	.650	44800±700		13.05	.920
"	1°	.649	48800±200		15.46	1.092
"	0°	.649	48300±300		15.14	1.070
"	0°	.649	47400±200		14.58	1.030
"	1°	.650	46400±200		13.99	.987
"	1°	.650	45900±300		13.69	.966
"	3°	.651	46100±200		13.84	.974
"	30°	.652	43800±500		12.51	1.025
"	30°	.652	45400±200		13.44	1.101
"	30°	.652	45800±200		13.68	1.120
"	30°	.652	45000±200		13.20	1.081
"	30°	.652	44000±500		12.62	1.034
"	30°	.652	43000±800		12.06	.987
116000	1°	1.387	53300±300	53000	38.4	1.080
"	30°	.659	43200±200	43000	12.18	.985
113000	2°	.510	48300±200	48600	12.04	1.151
119000	1°	.944	50800±300	50200	23.8	1.062
"	2°	.455	45800±200		9.54	1.064
"	30°	.455	40700±200		7.54	.980
"	35°	.460	39800±200		7.29	.985
"	45°	.460	41600±200		7.96	1.115
"	5°	.457	33000±1000		4.98	.555
"	3°	.454	30300±500		4.17	.466
"	0°	.456	30900±200		4.35	.565
"	0°	.459	26800±500		3.30	.363

Table VI - (Continued)

Tensile Strength	θ	$\frac{\epsilon}{d}$	Uncorrected $F(\frac{\epsilon}{d},\theta)$	Corrected $F(\frac{\epsilon}{d},\theta)$	$(10^{-8})U(\frac{\epsilon}{d},\theta)$	$(1+\sigma)(1+\omega)$
124000	30°	.347	39000±200		5.28	1.036
117000	4°	.673	48600±100	48300	15.70	1.063
"	.5°	.326	40300±300		5.29	.985
"	30.5°	.673	44100±500	43900	12.97	1.026
"	30°	.326	34900±200		3.97	.862
118000	0°	.206	34300±100		2.42	1.061
"	0°	.207	34900±200		2.52	1.092
"	45°	.206	29200±500		1.76	.973
"	45°	.206	23400±200		1.13	.625
132000	5°	1.375	55000±800	52400	37.8	1.053
119000	3°	.541	46500±200		11.70	1.038
"	30°	.540	42000±800		9.52	.986
"	3°	.260	35800±200		3.33	.931
"	8°	.259	33800±200		2.96	.843
"	28.5°	.260	33500±500		2.92	.936
"	44.5°	.263	31500±1000		2.61	.915
115000	30°	.662	43900±200	43900	12.76	1.023
"	30°	.662	41100±300	41100	11.18	.897
"	31°	.656	≥39300	>39300	>10.13	>.831

Table VI - (Continued)

Tensile Strength	θ	$\frac{e}{d}$	Uncorrected $F(\frac{e}{d},\theta)$	Corrected $F(\frac{e}{d},\theta)$	$(10^{-e})U(\frac{e}{d},\theta)$	$(1+\sigma)(1+\omega)$
85000	0°	.657	43700±200	48500	15.45	1.074
"	20°	.660	40000±200	44400	13.01	.932
"	29.8°	.657	37900±200	42100	11.64	.941
119000	30°	.650	38800±1000		9.78	.803
"	30°	.658	41800±200		11.50	.930
106000	1°	.827	48900±200	50300	20.9	1.100
132000	3°	.431	42800±500		7.90	.950
"	0°	.429	27600±200		3.27	.395
130000	0°	1.036	50900±400		26.8	1.070
"	1°	.505	46100±300		10.73	1.040
123000	.5°	.669	47000±200	46600	14.53	.987
"	1°	.673	29000±1000	28800	5.58	.377
127000	1°	1.055	49500±400	47800	24.1	.940
108000	0°	1.36	49500±200	50600	34.8	.984
"	0°	1.39	50800±200	51900	37.4	1.031
"	0°	1.39	51200±500	52300	38.0	1.048
"	0°	1.39	50900±200	52000	37.6	1.036
"	0°	1.39	47900±500	48900	33.2	.916
"	0°	1.365	47200±200	48200	31.7	.890
109000	1.5°	.980	45500±200	46300	21.0	.896

Table VI - (Continued)

Tensile Strength	θ	$\frac{e}{d}$	Uncorrected $F(\frac{e}{d},\theta)$	Corrected $F(\frac{e}{d},\theta)$	$(10^{-6})U(\frac{e}{d},\theta)$	$(1+\sigma)(1+\omega)$
116000	0°	1.63	53000±500	53000	45.8	1.023
"	.5°	1.615	53200±200	53200	45.7	1.035
"	.5°	1.62	50700±500	50700	41.6	.940
97000	4.5°	1.69	52300±300	55400	51.9	1.113
"	3°	.819	46100±200	48800	19.50	1.042
"	20°	.823	44400±300	47000	18.18	1.028
"	30°	.823	43700±500	46300	17.64	1.087
121000	0°	1.016	49400±500	48500	23.9	.976
"	1°	1.02	50000±1000	49100	24.6	.999
101000	0°	1.35	48700±100	50900	35.0	1.000
101000	0°	1.35	49700±200	51900	36.4	1.040

Table VII - Plate Penetration Coefficients for AP Bombs vs Class B Plate corrected for tensile strength to 115000 (lb)/(in)^2 Tensile Strength at 15°C.

Bomb	Plate Number	Tensile Strength	θ	$\frac{e}{d}$	Uncorrected $F(\frac{e}{d},\theta)$	Corrected $F(\frac{e}{d},\theta)$	$(10^{-6})U(\frac{e}{d},\theta)$	$(1+\sigma)(1+\omega)$	$e^{-\frac{1}{8}h^2(s_b^0-s_b^m)^2}$	$\cos\theta$
12" SAP M58A1	X8651	121000	21°	.160	≥ 26200		>1.10	> .85		.934
12.2" SAP T5	3A737A1	107000	20°	.162	≤ 36000	<36900	<2.20	<1.66		.940
"	"	"	20°	.328	37000±1000	37900	4.71	.93	.88	.940
12" AP Mk 33	8372	110000	20°	.396	38000±2000	38700	5.94	.865	.66	.940
"	KK148	109000	25°	.461	≤ 41500	<42400	<8.30	<1.010		.906
"	"	"	29°	.460	≤ 42100	<43000	<8.51	<1.080		.875
"	"	"	24.5°	.463	41400±300	42300	8.29	1.000	.99	.910
"	"	"	30°	.463	41000±200	41900	8.14	1.034	.99	.866
"	KK203	113000	19.5°	.484	43500±200	44000	9.38	1.023	.99	.943
"	"	"	30°	.484	≤ 38600	<39000	<7.36	< .88		.866
"	KK719	113000	30°	.273	33000±200	33200	3.01	.895	.99	.866
"	TT813	113000	30.5°	.273	31000±700	31200	2.66	.795	.91	.862
"	53C425A1	113000	29.5°	.417	≤ 38500		<6.19	< .904		.870
"	53C164A1	106000	20°	.479	≤ 42400	<43400	<9.02	<1.004		.940
"	35E601A1	115000	30°	.266	31200±300	31200	2.99	.809	.99	.866
"	33G051A1	114000	29.5°	.261	30900±300	31000	2.49	.809	.99	.870
14" AP C-20	5A457A3	106000	15°	.378	40000±500	40900	6.32	.962	.97	.966

Table VII - (Continued)

Bomb	Plate Number	Tensile Strength	θ	$\frac{e}{d}$	Uncorrected $F(\frac{e}{d},\theta)$	Corrected $F(\frac{e}{d},\theta)$	$(10^{-8})U(\frac{e}{d},\theta)$	$(1+\sigma)(1+\omega)$	$e^{-\frac{1}{2}k^2(\sigma_R^2-\sigma_E^2)^2}$	$\cos\theta$
14" AP Mk 1	8943	103000	20.5°	.500	43000±700	44700	8.99	1.056	.94	.937
"	"	"	24.5°	.500	40400±200	42000	8.82	.958	.99	.910
"	"	"	30°	.504	37600±200	39100	7.70	.870	.99	.866
"	"	"	29.5°	.502	40200±500	41800	8.77	.990	.97	.870
"	KK834	112000	25°	.397	39000±1000	39300	8.14	.923	.89	.906
"	3B427A3	112000	25°	.407	$\leq$ 40500	<41100	<8.88	<1.000		.906
"	4B586A3	112000	25°	.401	36500±200	37000	5.49	.819	.99	.906
"	31C177A1	106000	29.5°	.464	39200±200	40400	7.57	.952	.99	.870
"	"	"	29.5°	.464	$\geq$ 39000	>40200	>7.50	> .943		.870

VII

REFERENCES

(Ballistic Data)

(1) "Armor Penetration of cal .60 Bullets of Various Contours", H. W. Zuker and T. A. Read, Frankford Arsenal Report No. R-615. (May, 1945)

(2) "The effect of the shape of the head of AP shot on critical velocities for penetration at normal" R. MacPhail, Proof and Development Establishment, Valcartier, P. Q. Canada (May 1943). "Second Progress Report on the Investigation of Scale Effect in Armour Penetration. Effect of Hardness on Plate Performance". D. G. Sopwith, A. F. C. Brown, and V. M. Hickson, National Physical Laboratory Report No. 50 (February, 1943). "Third Progress Report on the Investigation of Scale Effect in Armour Penetration. Firing Trials at Normal attack with geometrically similar Shot against Homogeneous Armour of varied Hardness." A. F. C. Brown and V. M. Hickson, National Physical Laboratory Report No. 79 (September, 1944).

(3) "Penetration of Homogeneous Armor by 3" Flat Nosed Projectiles" NPG Report No. 7-43 (April 1943). "The Effect of Nose Shape on Ballistic Performance of 15 lb. 3" AP Solid Shot Against Homogeneous Armor Plate", NPG Report No. 2-43.

(4) "Ballistic Summary. Part I. The Dependence of Limit Velocity on Plate Thickness and Obliquity at Low Obliquity". NPG Pamphlet Report No. 2-46 (March, 1946).

NPG PHOTO NO. 2975 (APL)

[redacted] UNCLASSIFIED

FIGURE (7)

THE PLATE PENETRATION COEFFICIENT FOR 0° OBLIQUITY

Standard Experimental Curve for 3" AP M79 Projectile vs STS of 115000 (lb)/(in)^2 Tensile Strength at 15°C

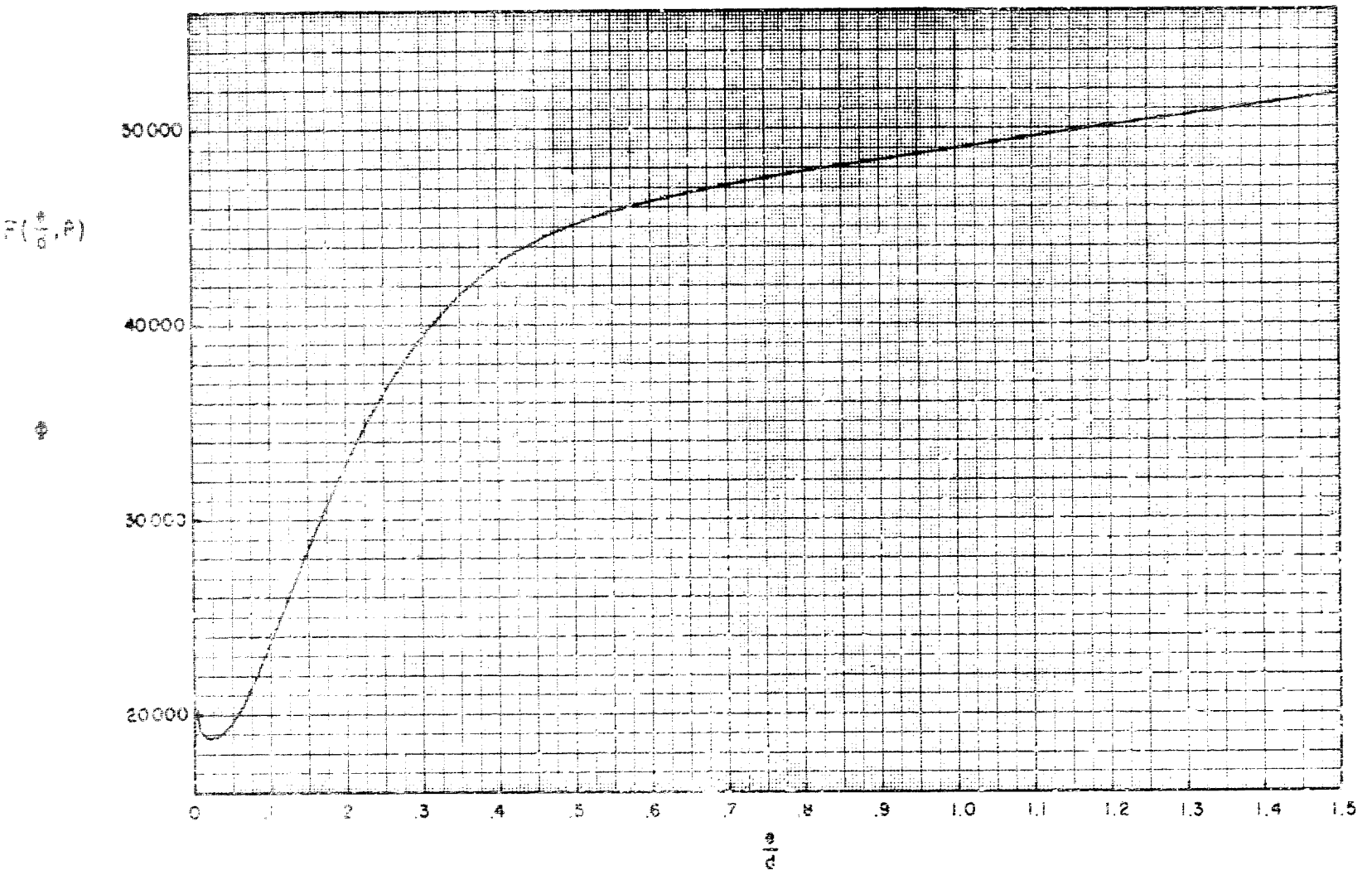

NPG PHOTO NO. 3027 (APL)

FIGURE (2)

THE OBLIQUITY FUNCTION Θ

3" AP M79 Projectile in Homogeneous Plate

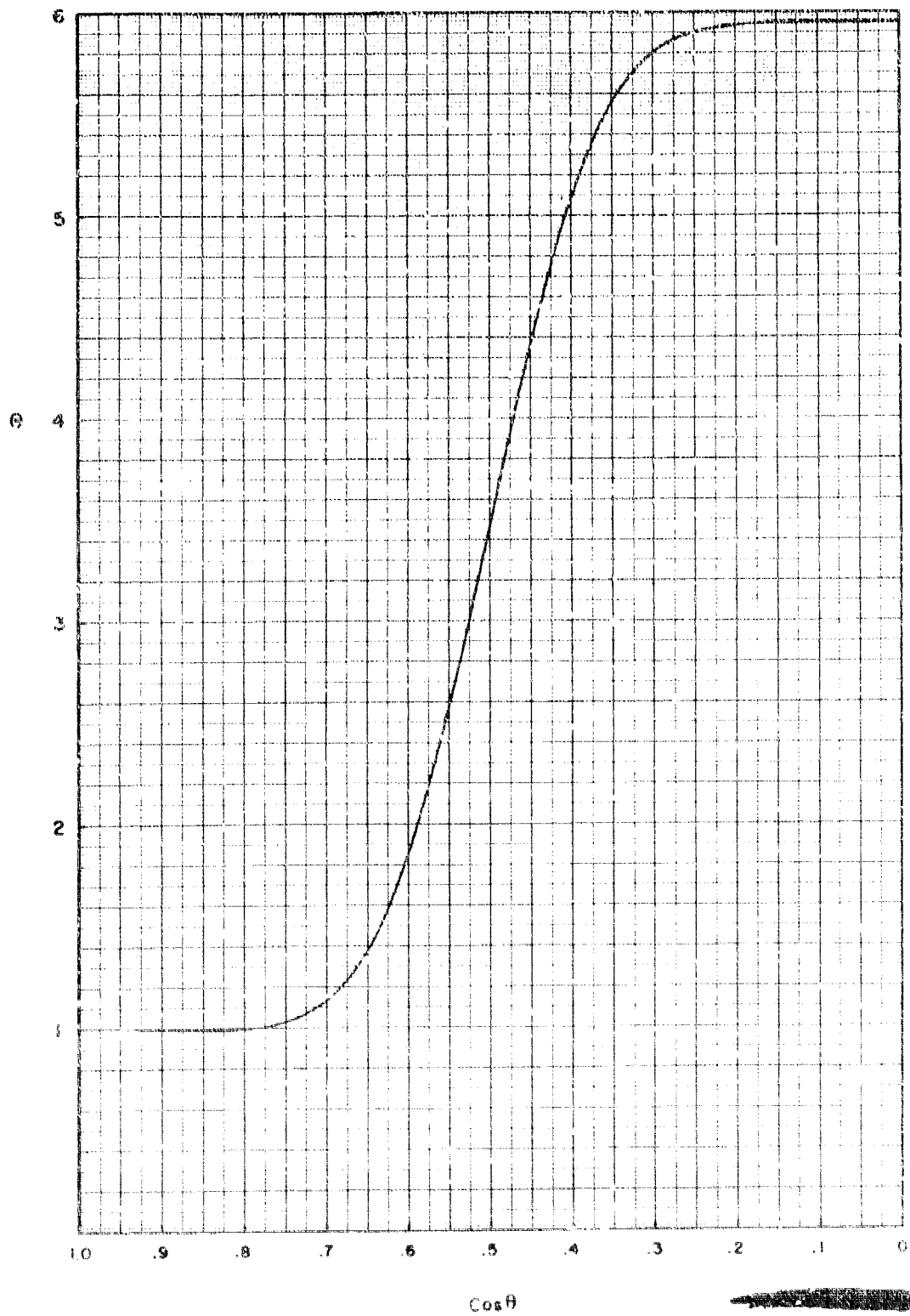

NPG PHOTO NO. 3028 (APL)

FIGURE (3)

CYLINDRICAL POLAR COORDINATES OF A PROJECTILE NOSE CONTOUR

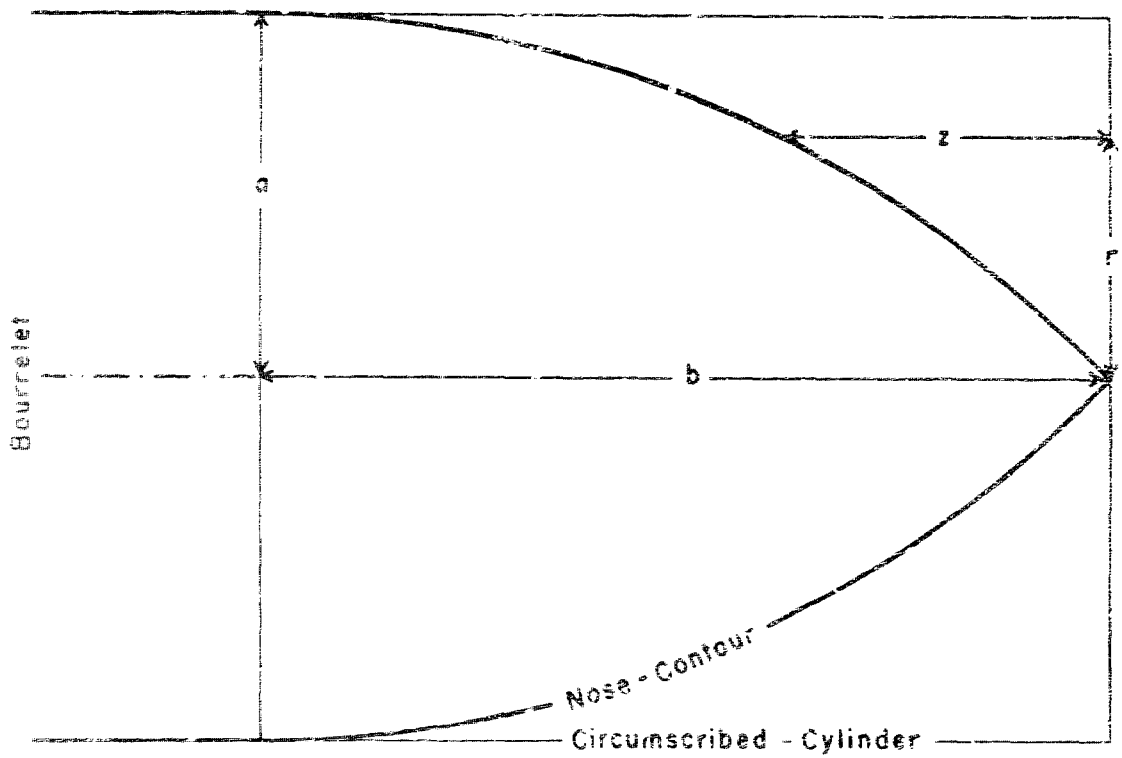

SPG PHOTO NO 3088 (APL)

PARAMETERS OF THE OGIVE

FIGURE (4)

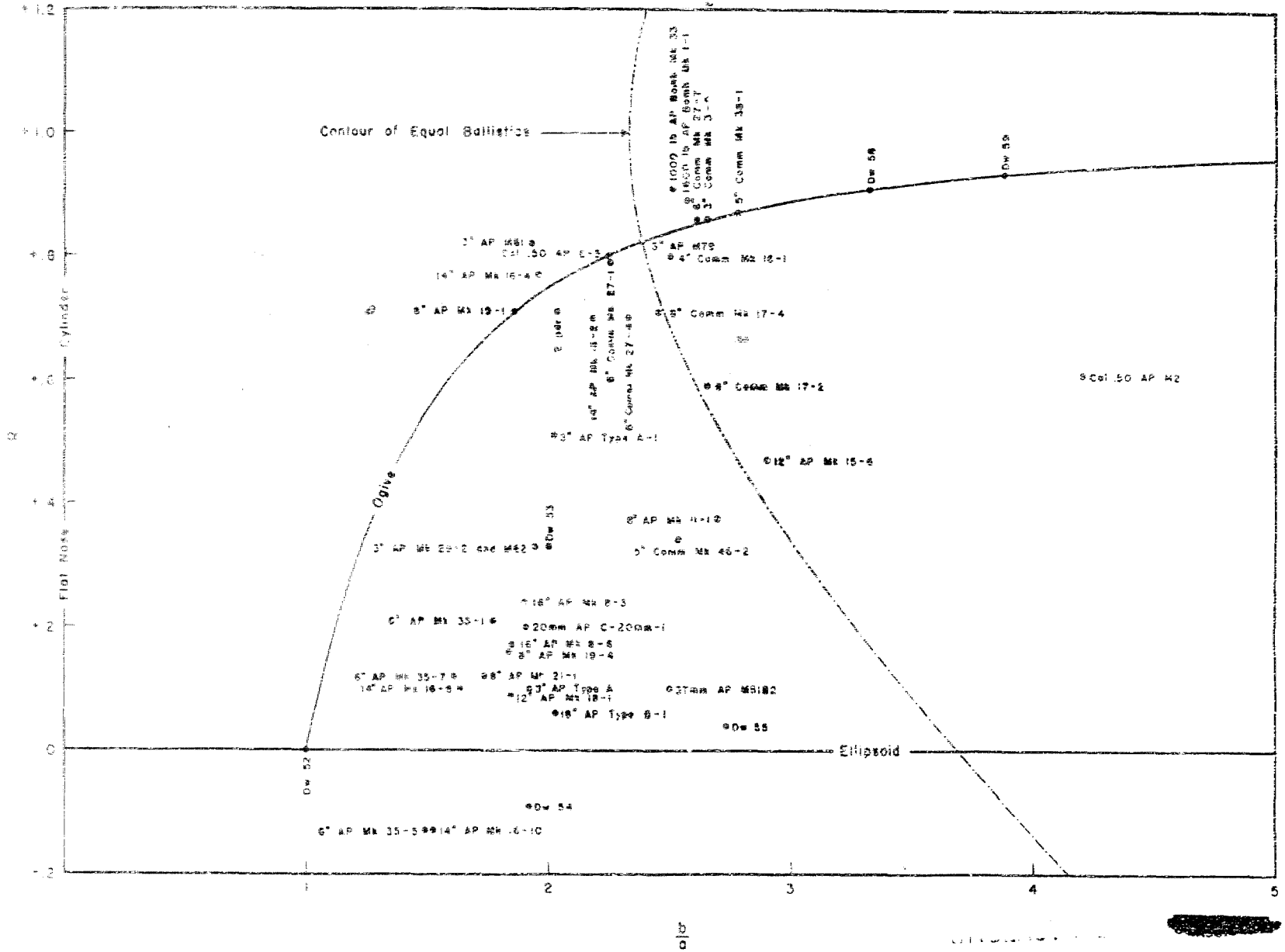

RPG PHOTO NO. 3030 (APL)

PROJECTILE NOSE CONTOURS

FIGURE (5)

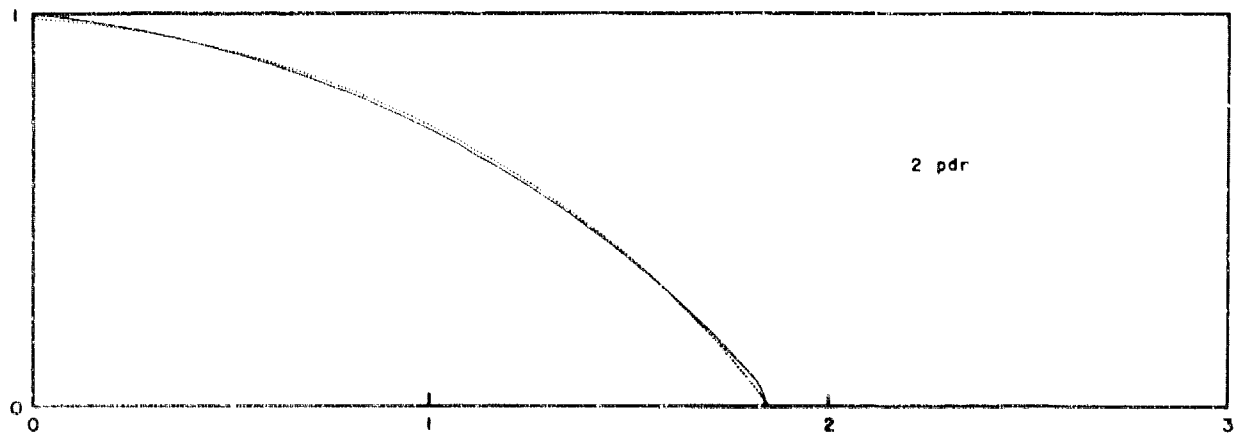

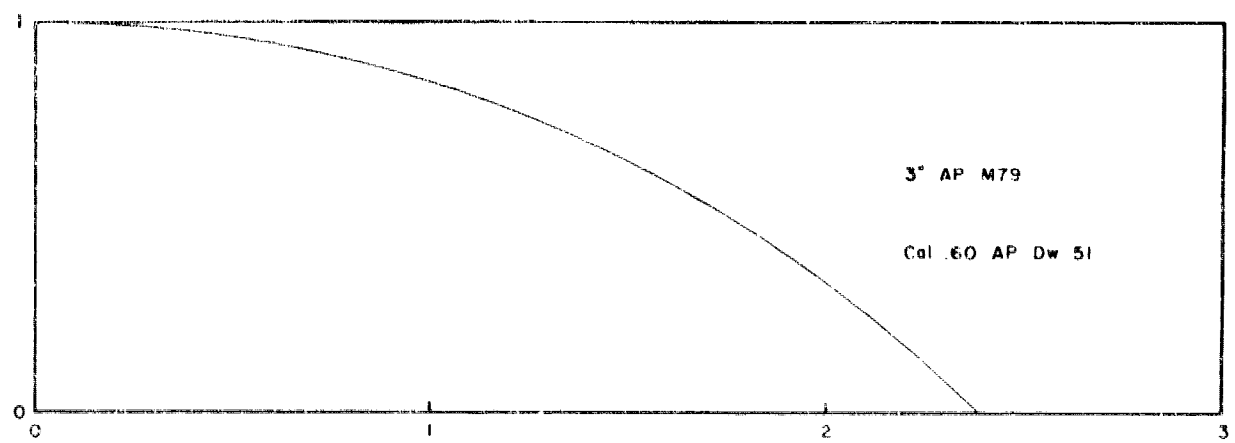

NPG PHOTO NO. 3031 (APL)

PROJECTILE NOSE CONTOURS

FIGURE (6)

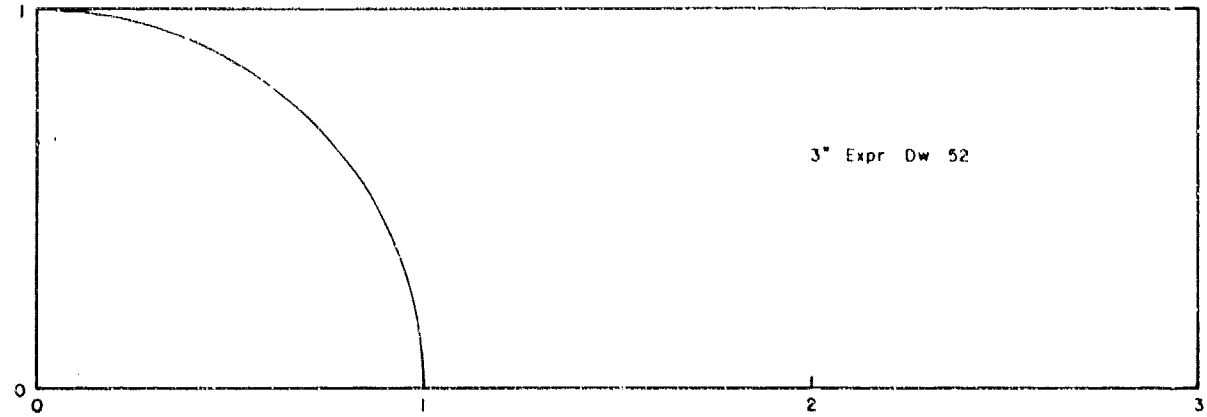

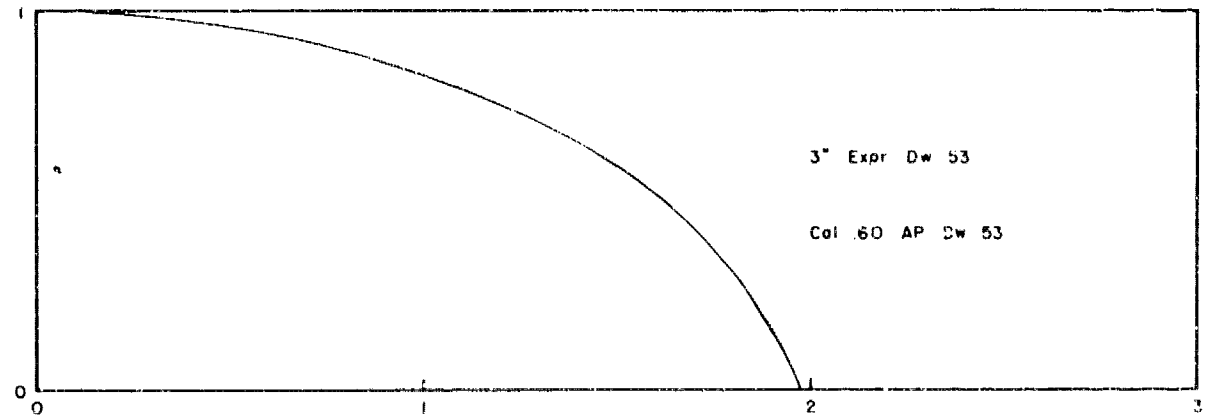

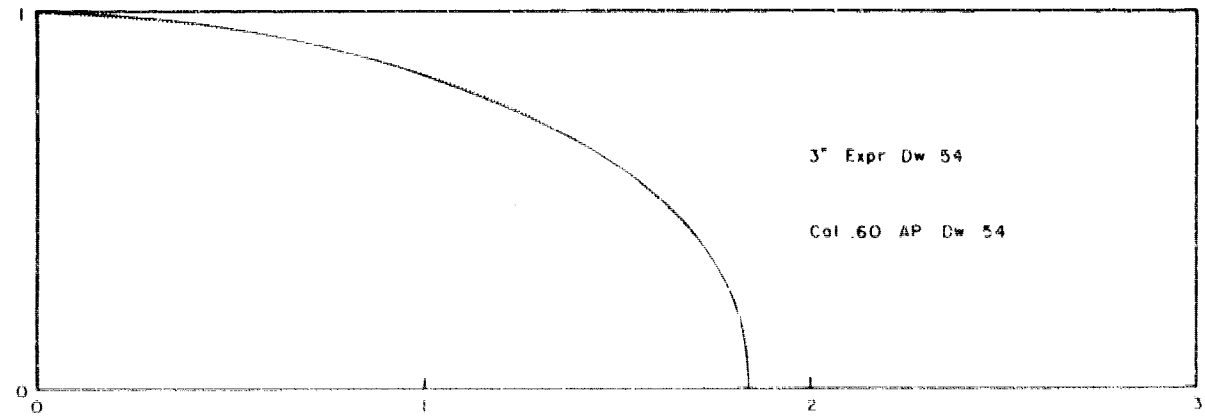

NPG PHOTO NO. 3032 (AFL)

PROJECTILE NOSE CONTOURS

FIGURE (7)

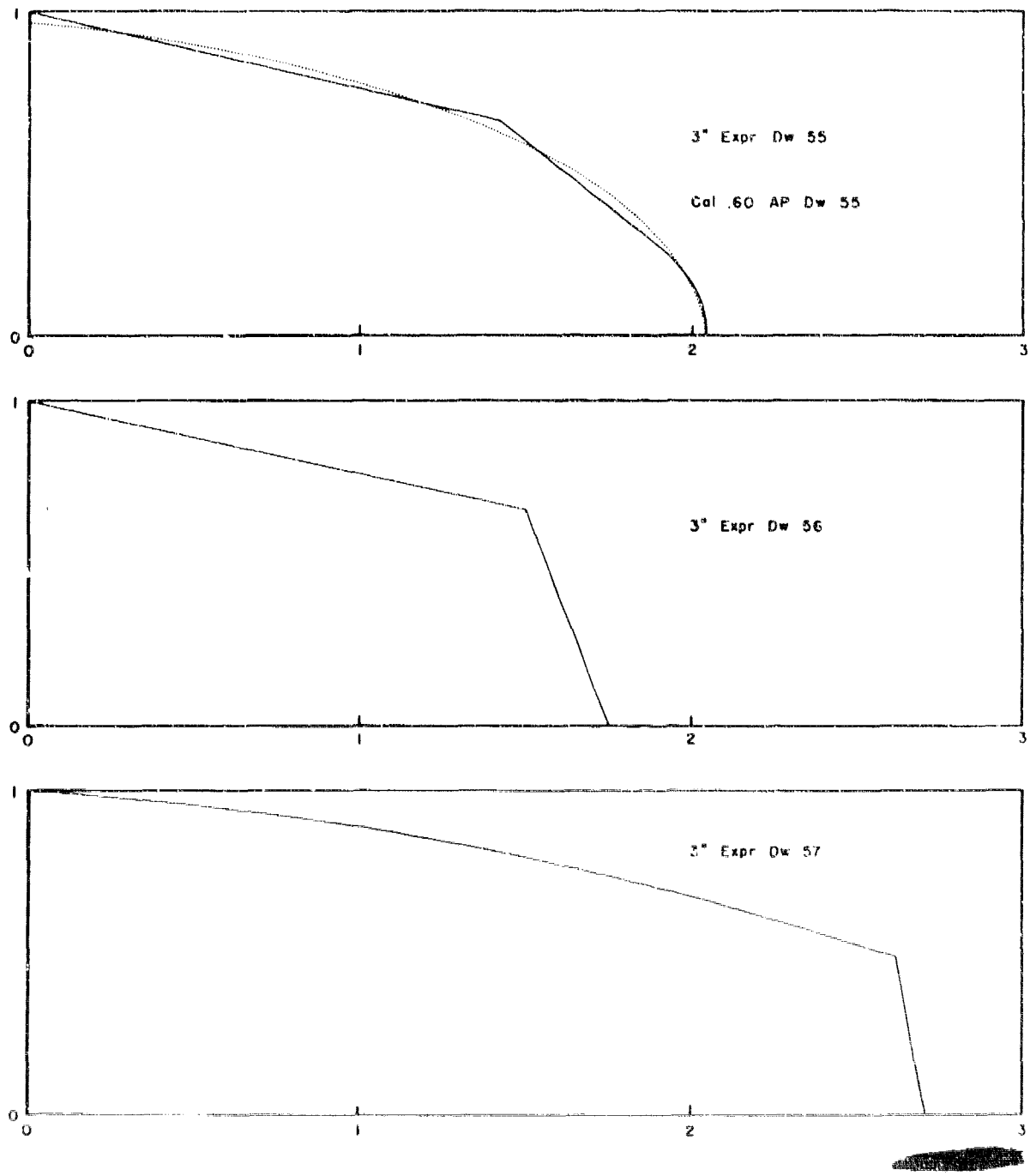

NPG PHOTO NO 3035 (APL)

PROJECTILE NOSE CONTOURS

FIGURE (8)

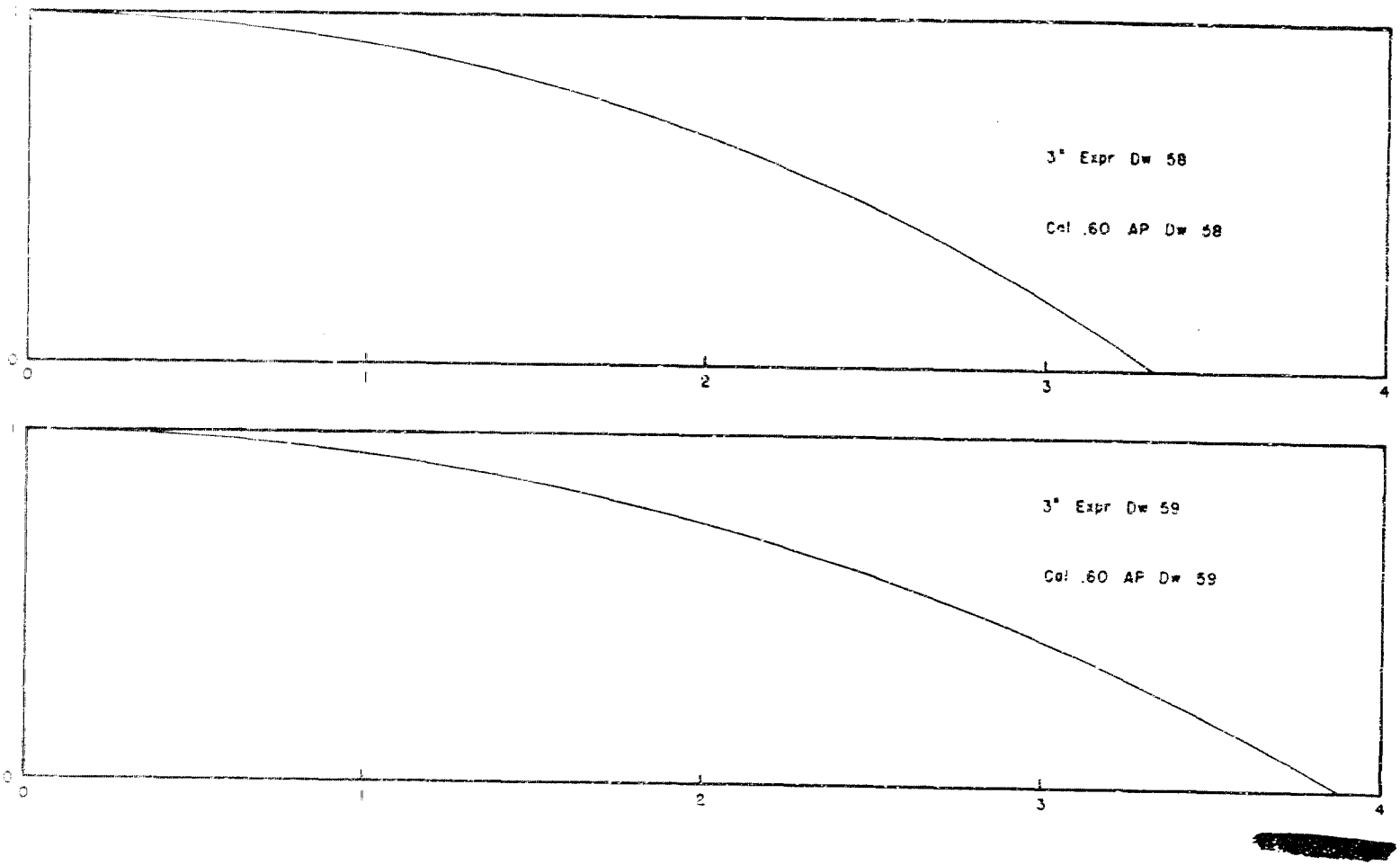

BPG PHOTO NO. 3034 (APL)

PROJECTILE NOSE CONTOURS

FIGURE (9)

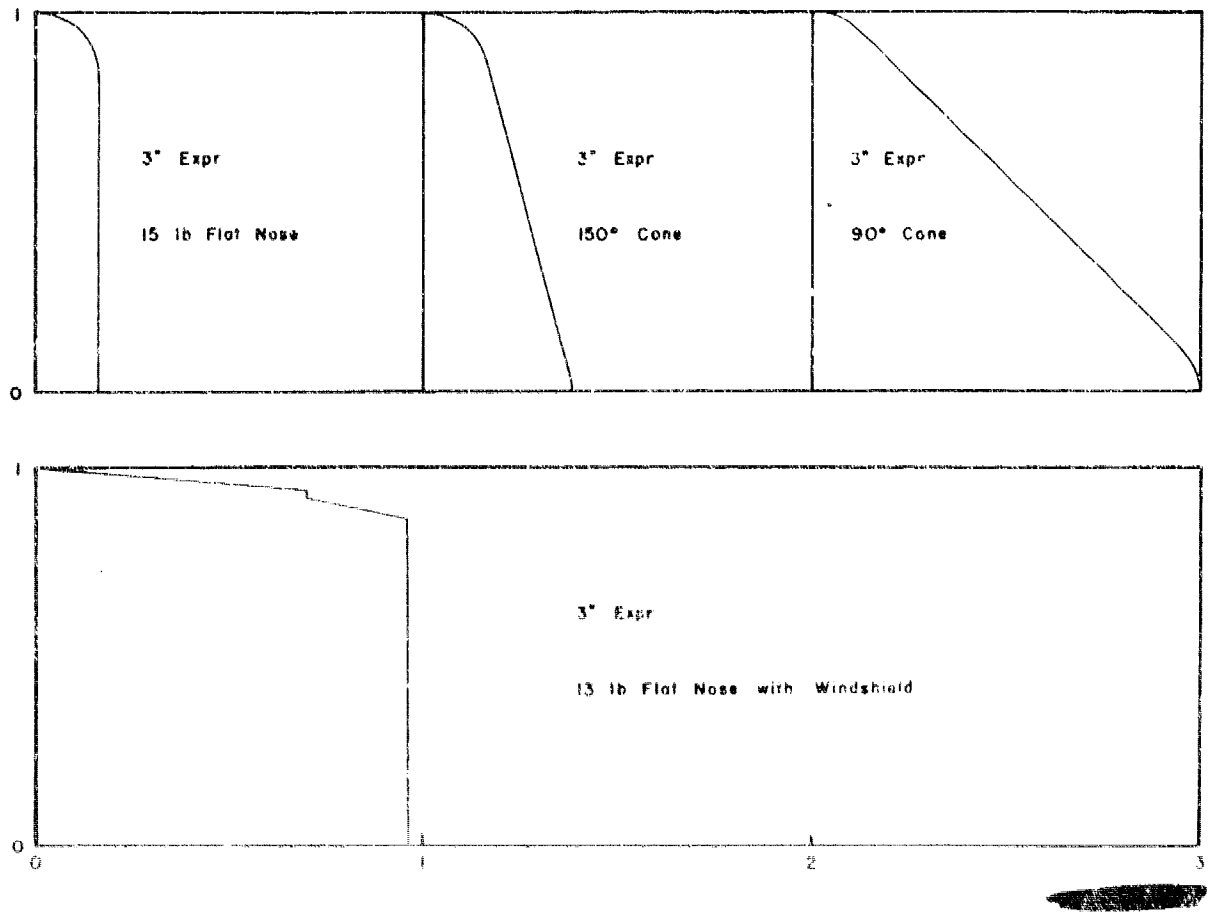

BPG PHOTO NO. 3035 (APL)

PROJECTILE NOSE CONTOURS

FIGURE (10)

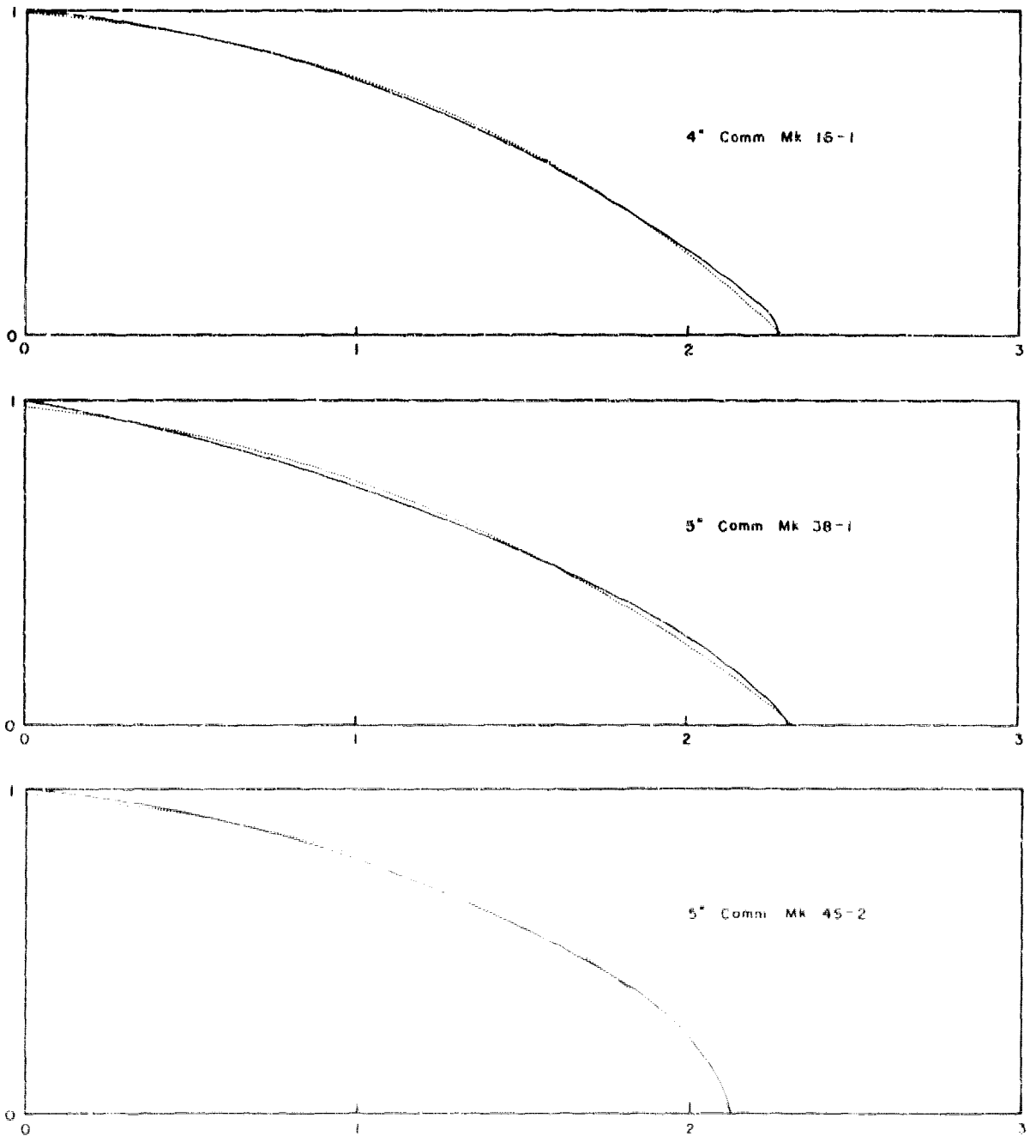

NPG PHOTO NO. 3036 (APL)

PROJECTILE NOSE CONTOURS

FIGURE (11)

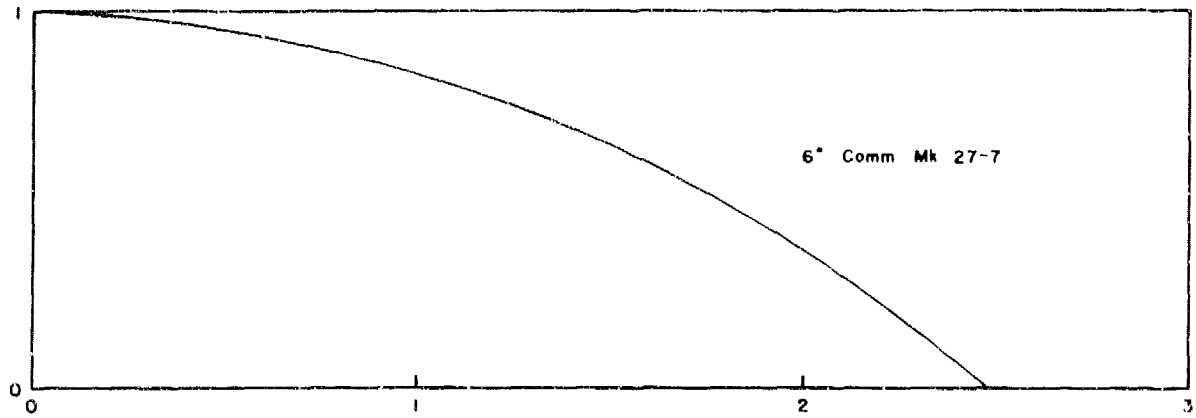

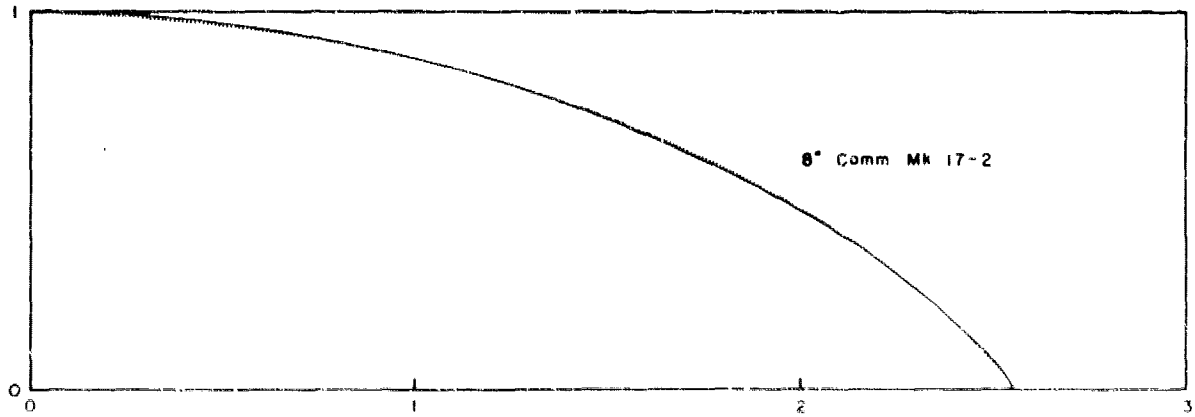

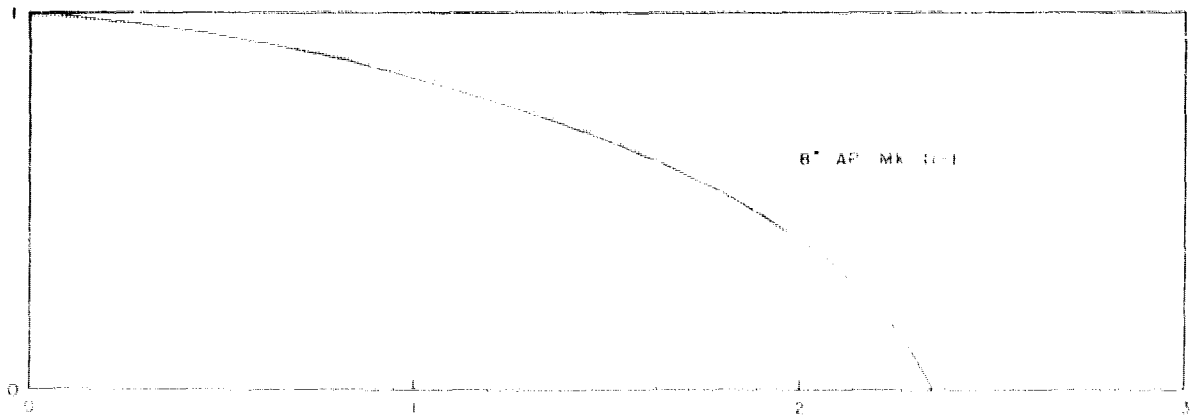

NPG PHOTO NO. 3037 (APL)

PROJECTILE NOSE CONTOURS

FIGURE (12)

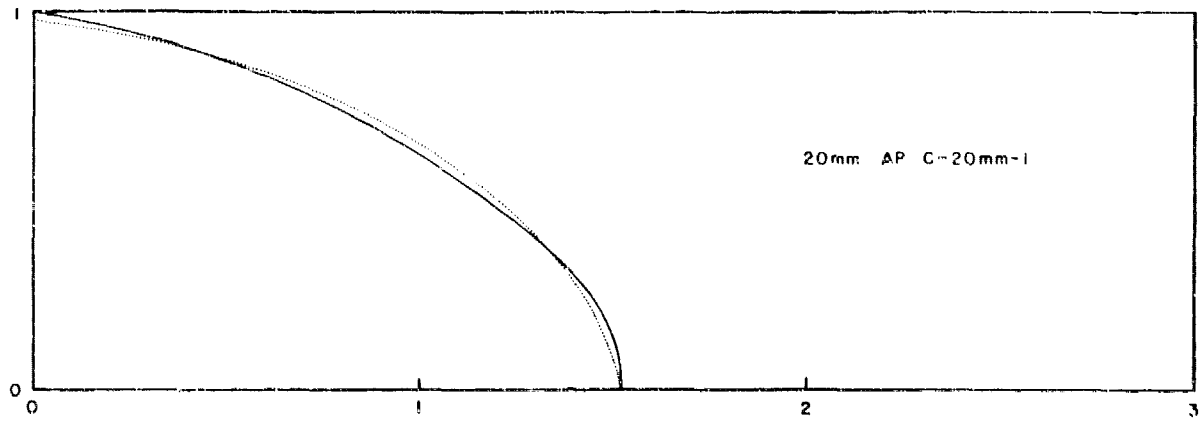

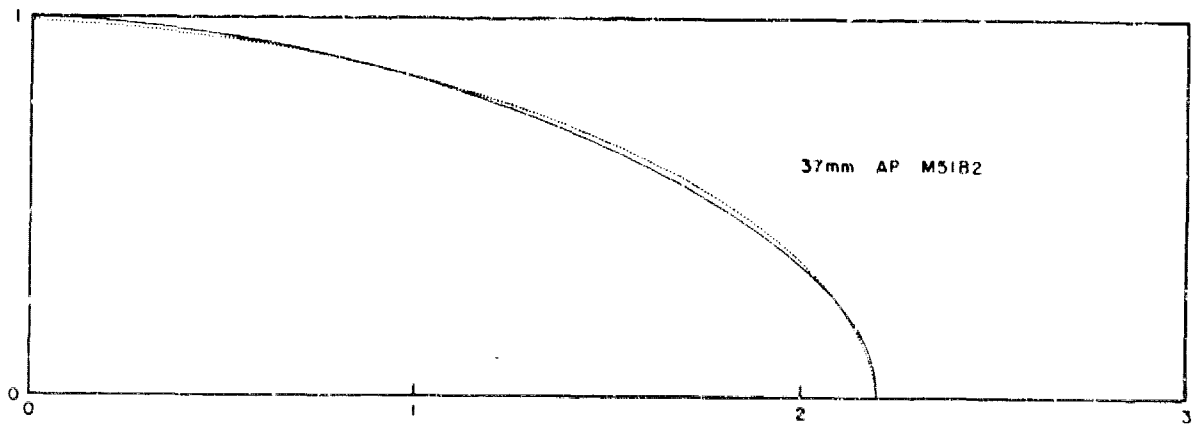

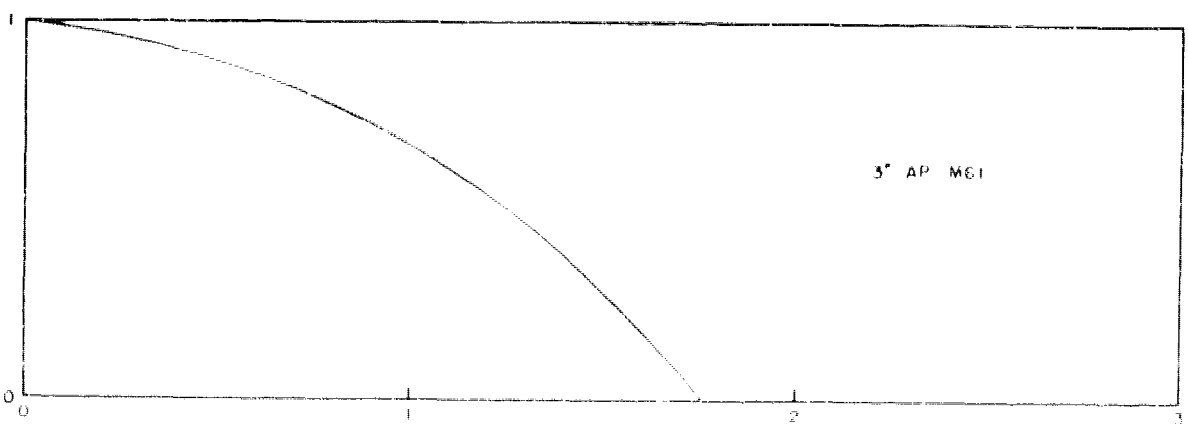

WPG PHOTO NO. 3038 (APL)

PROJECTILE NOSE CONTOURS

FIGURE (13)

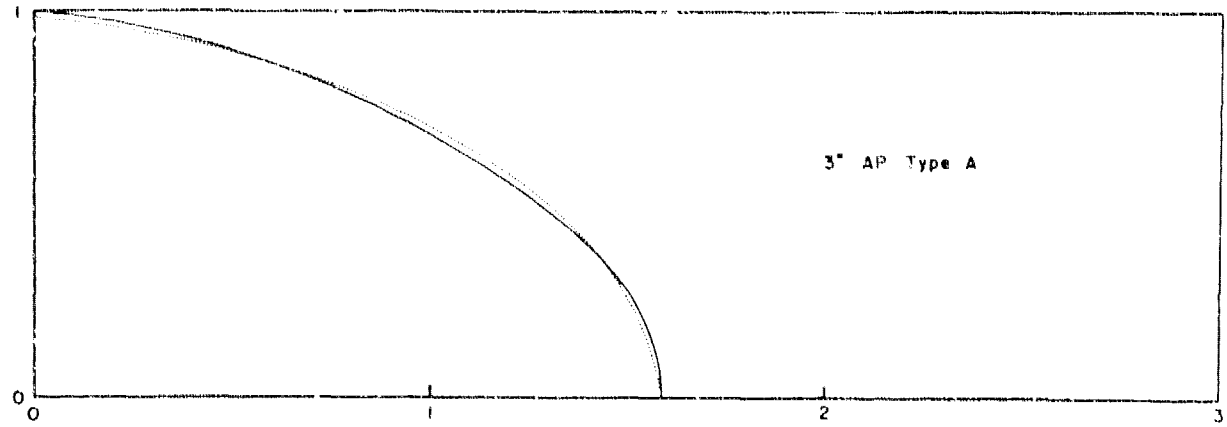

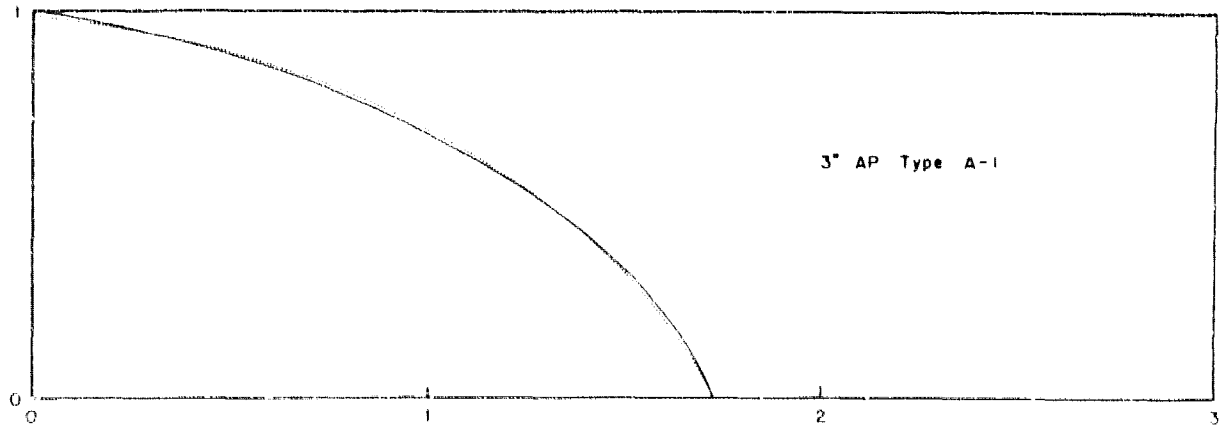

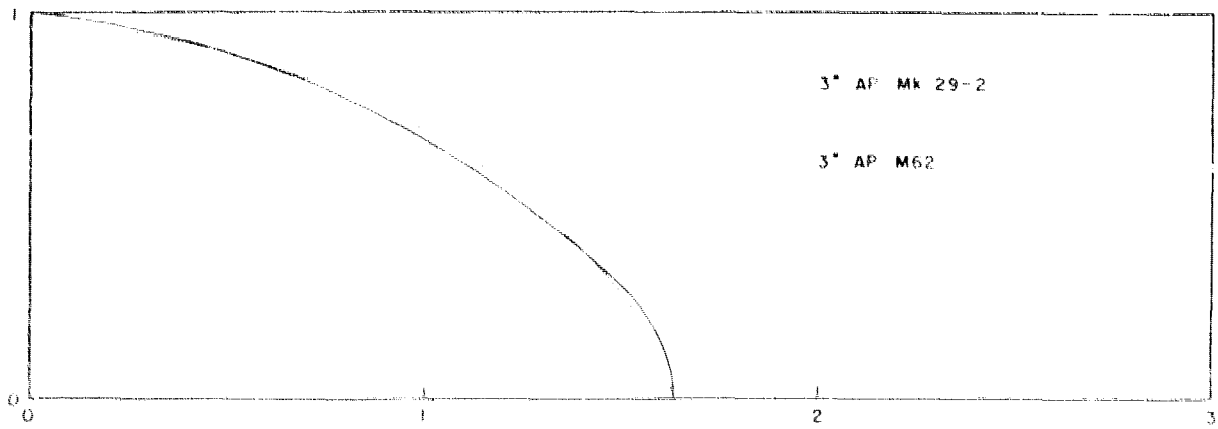

NPG PHOTO NO. 3038 (APL)

PROJECTILE NOSE CONTOURS

FIGURE (14)

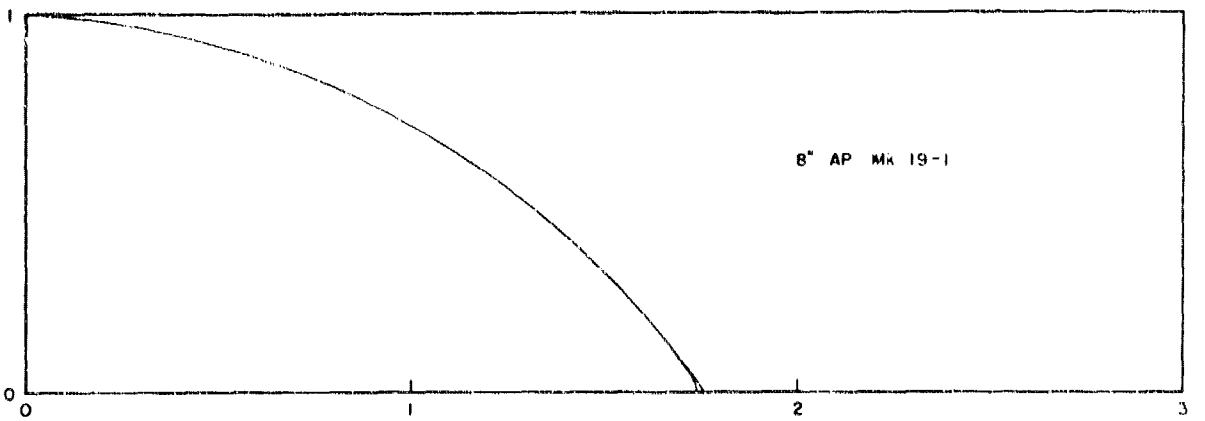

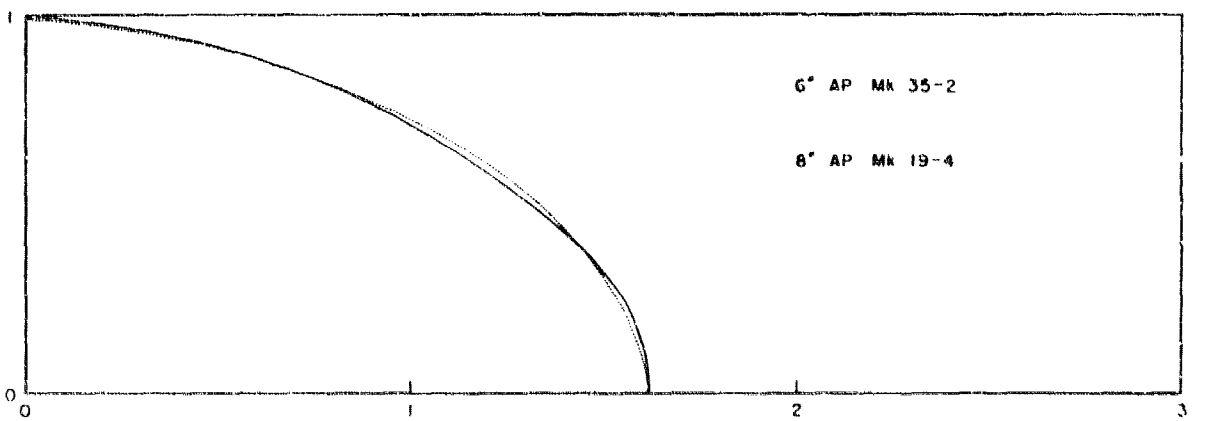

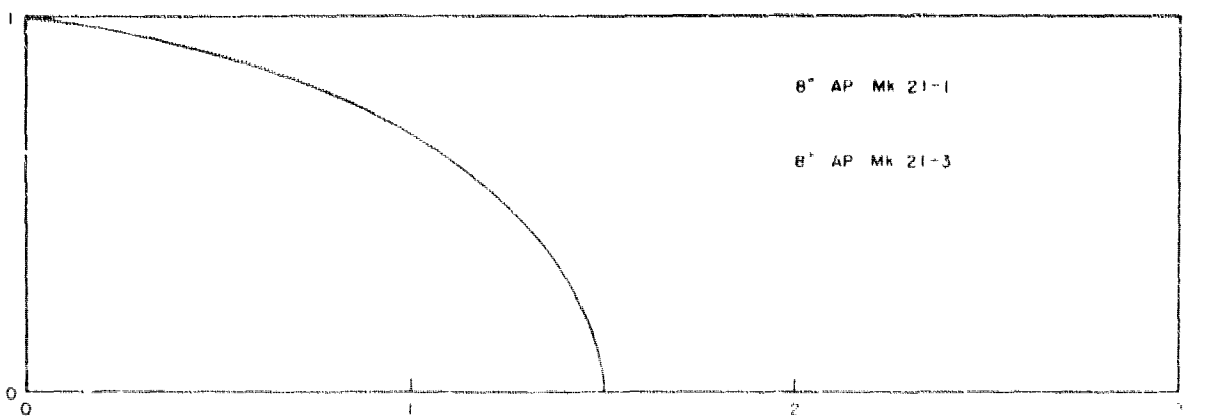

MP8 PHOTO NO. 3040 (APL

PROJECTILE NOSE CONTOURS

FIGURE (15)

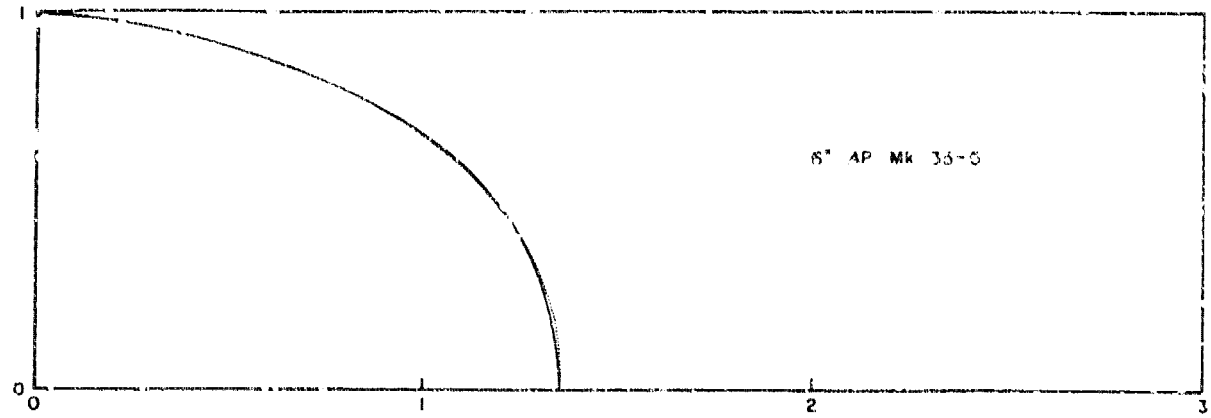

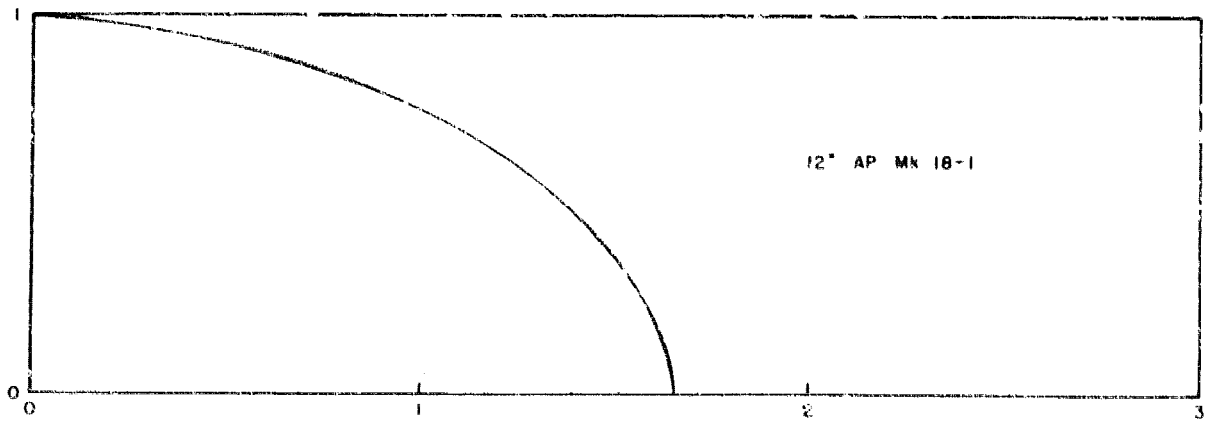

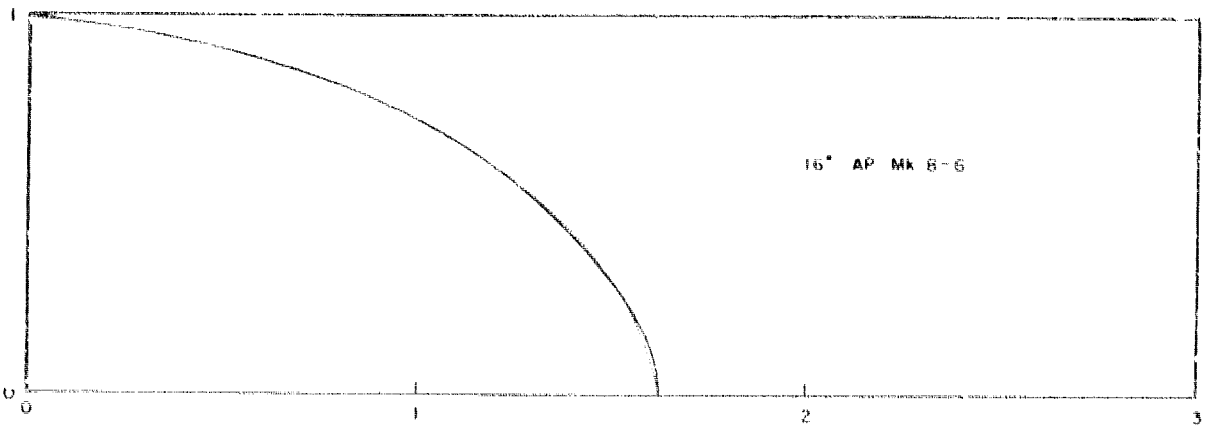

PROJECTILE NOSE CONTOURS

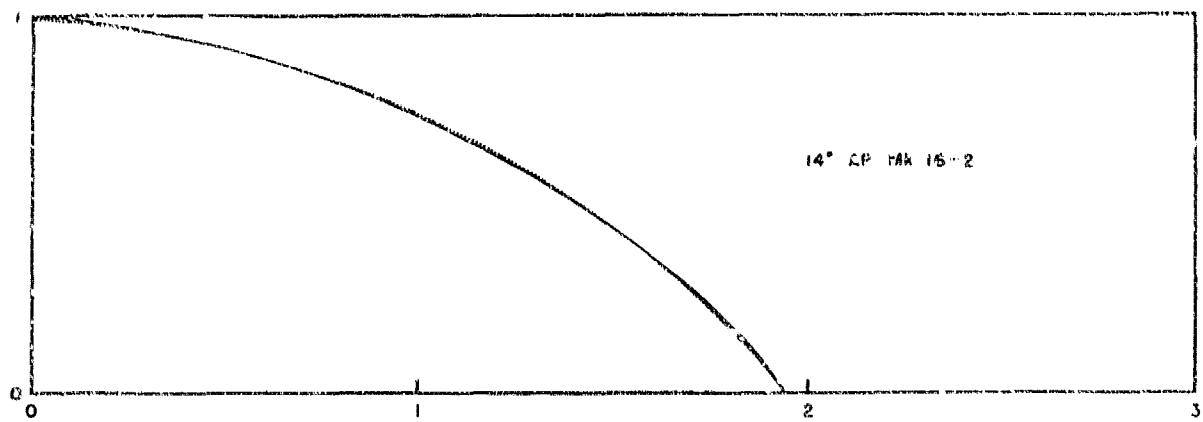

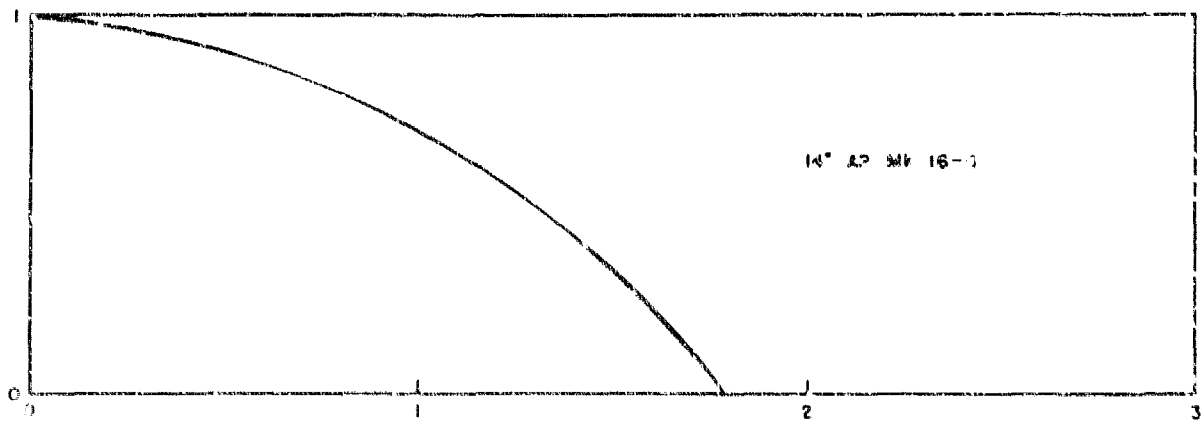

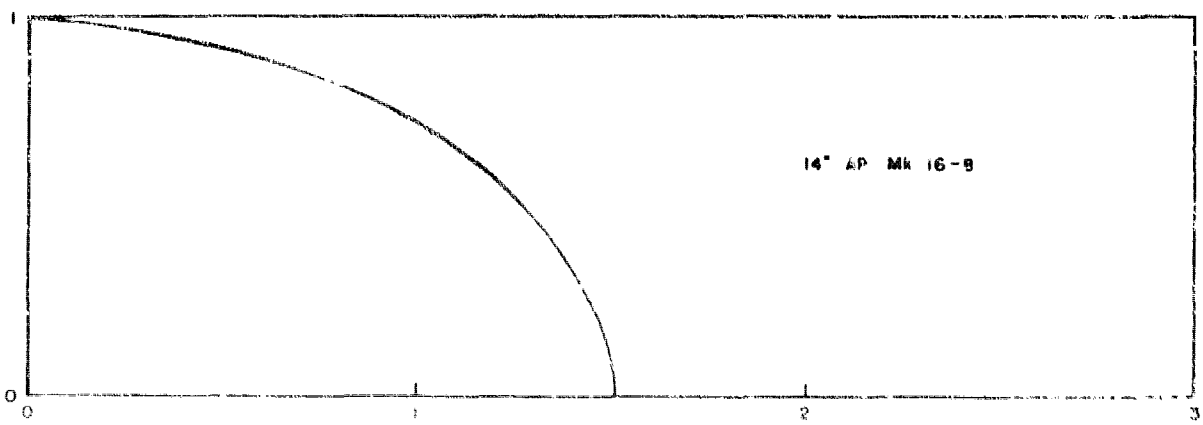

NPG PHOTO NO. 3043 (APL)

THE SCALE EFFECT

FIGURE 4(B)

Monobloc Projectiles vs Homogeneous Plate, corrected to 115000 $(lb)/(in)^2$ Static Tensile Strength

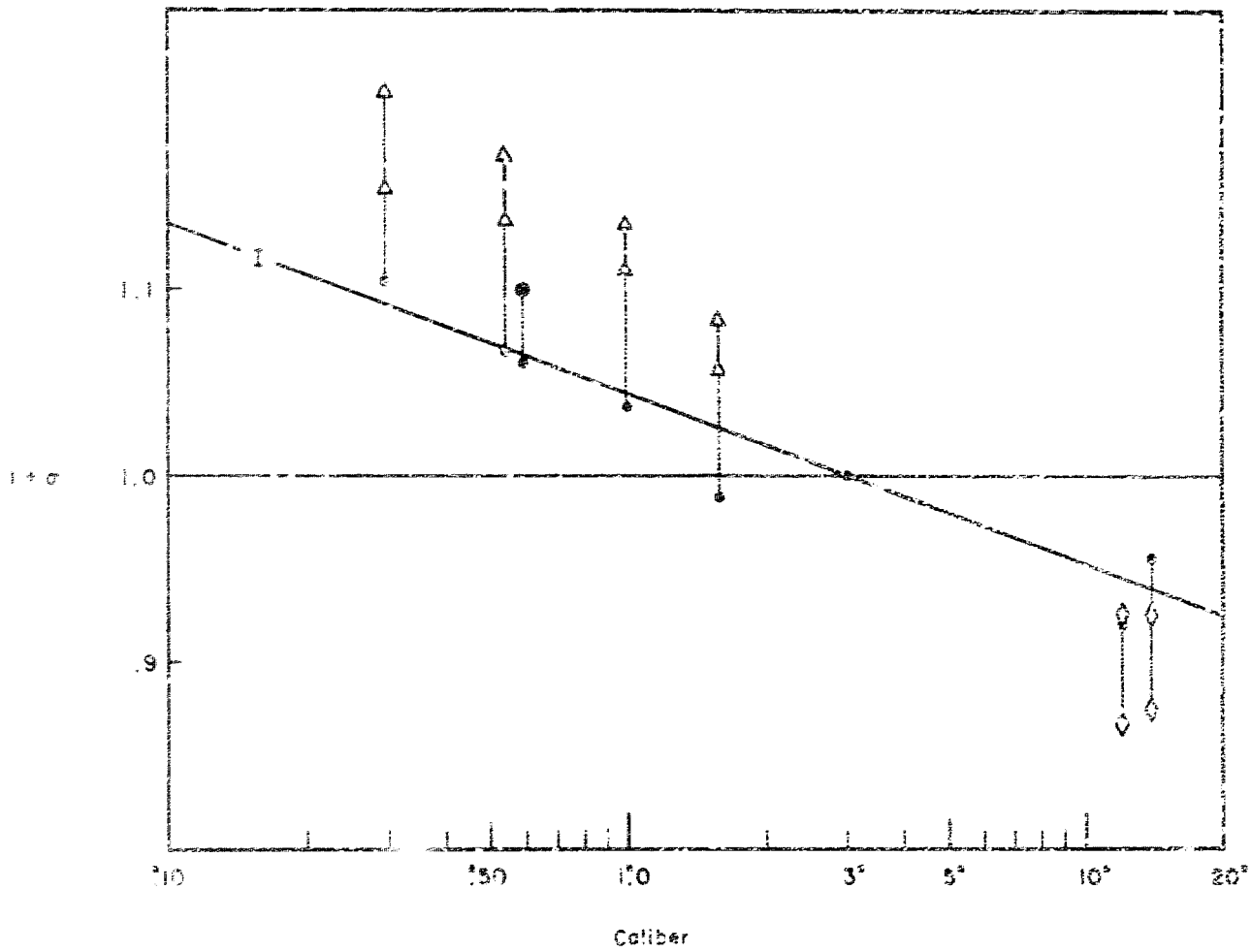

- Monobloc Projectiles, corrected
- Col .50 Expr Dw 51 Projectile, uncorrected
- Scale Model 2 pdr Projectile, "
- Major Caliber AP Bomb, "

CURVE I Basic Formula of NPG SR 550

$\sigma = -(.04)\log(4d)$

MPG PHOTO NO. 3044 (APL)

FIGURE (19.

THE DEPTH OF PENETRATION

Undeformed Projectiles in Homogeneous Plate at Low Obliquity

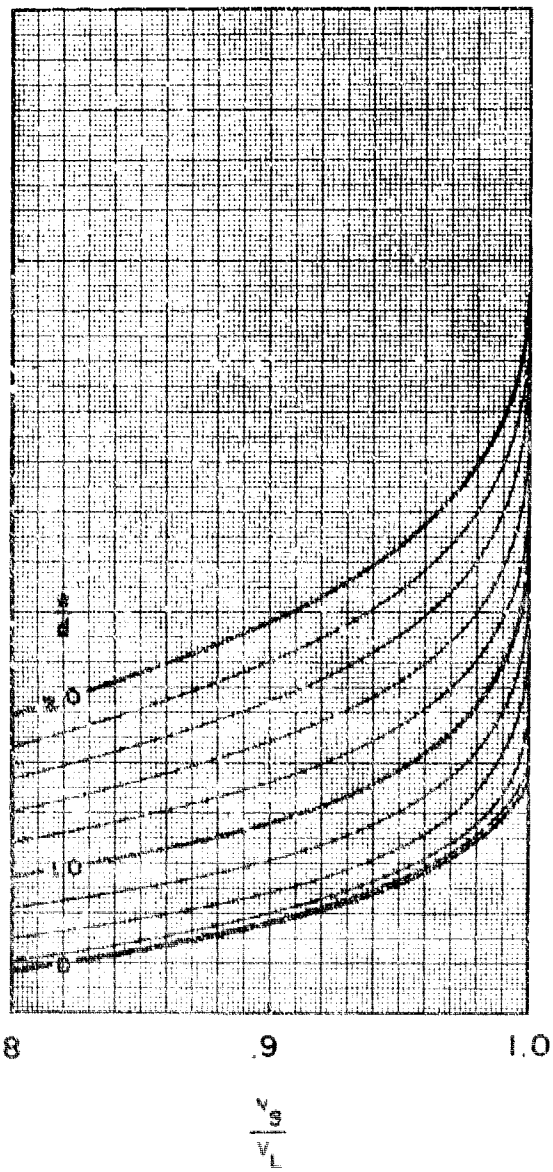

e = plate thickness

d = projectile diameter

p = depth of penetration

v_s = striking velocity

v_L = limit velocity

g = increase in p/d due to difference in nose shape

UNCLASSIFIED

[redacted]

NPG PHOTO NO. 3045 (APL)

FIGURE (2G)

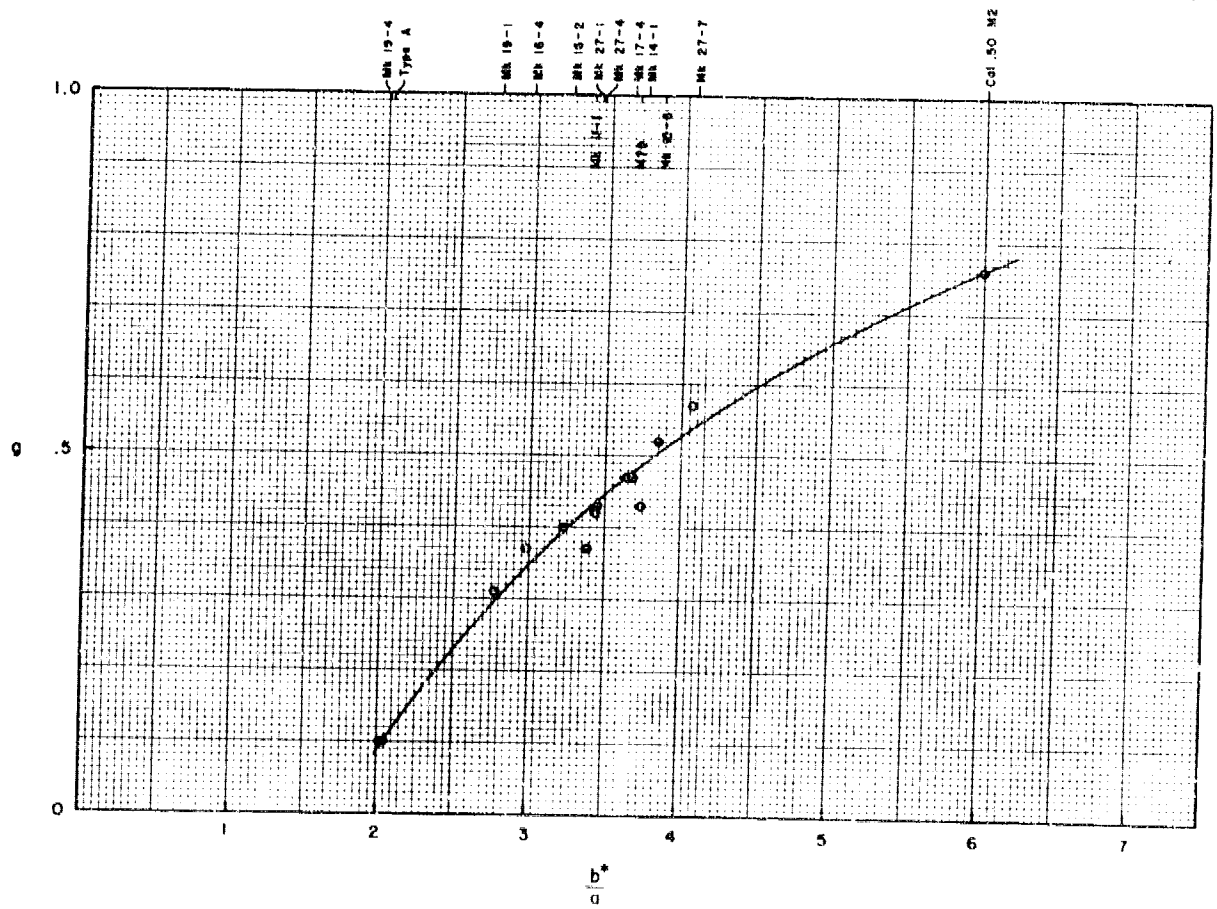

THE EFFECT OF NOSE SHAPE ON DEPTH OF PENETRATION IN HOMOGENEOUS PLATE

[redacted]

UNCLASSIFIED

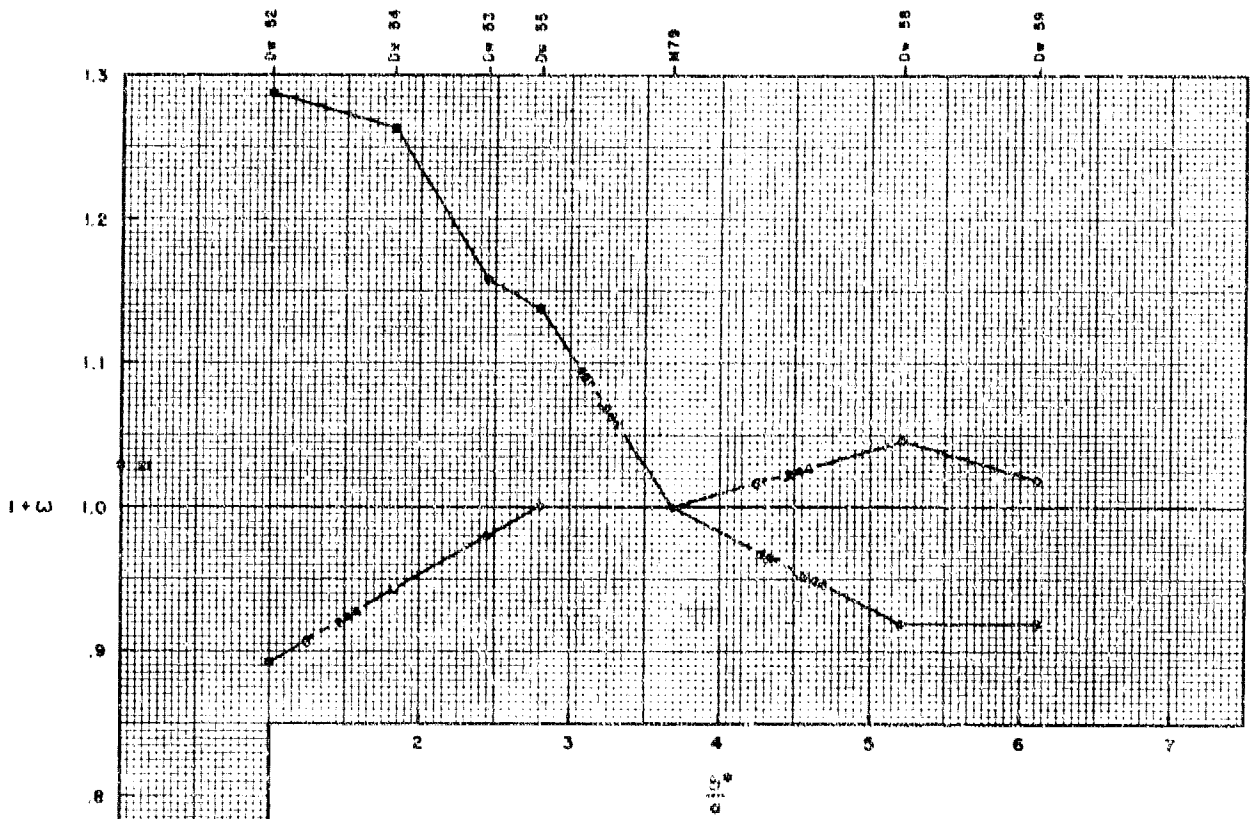

WPG PHOTO NO. 3048 (APL)

FIGURE (21)

THE OGIVE EFFECT

3" Monobloc Projectiles vs STS at e/d < .5

○ 3" Projectiles at 0° Obliquity

● " " " 45° "

e/d as indicated

UNCLASSIFIED

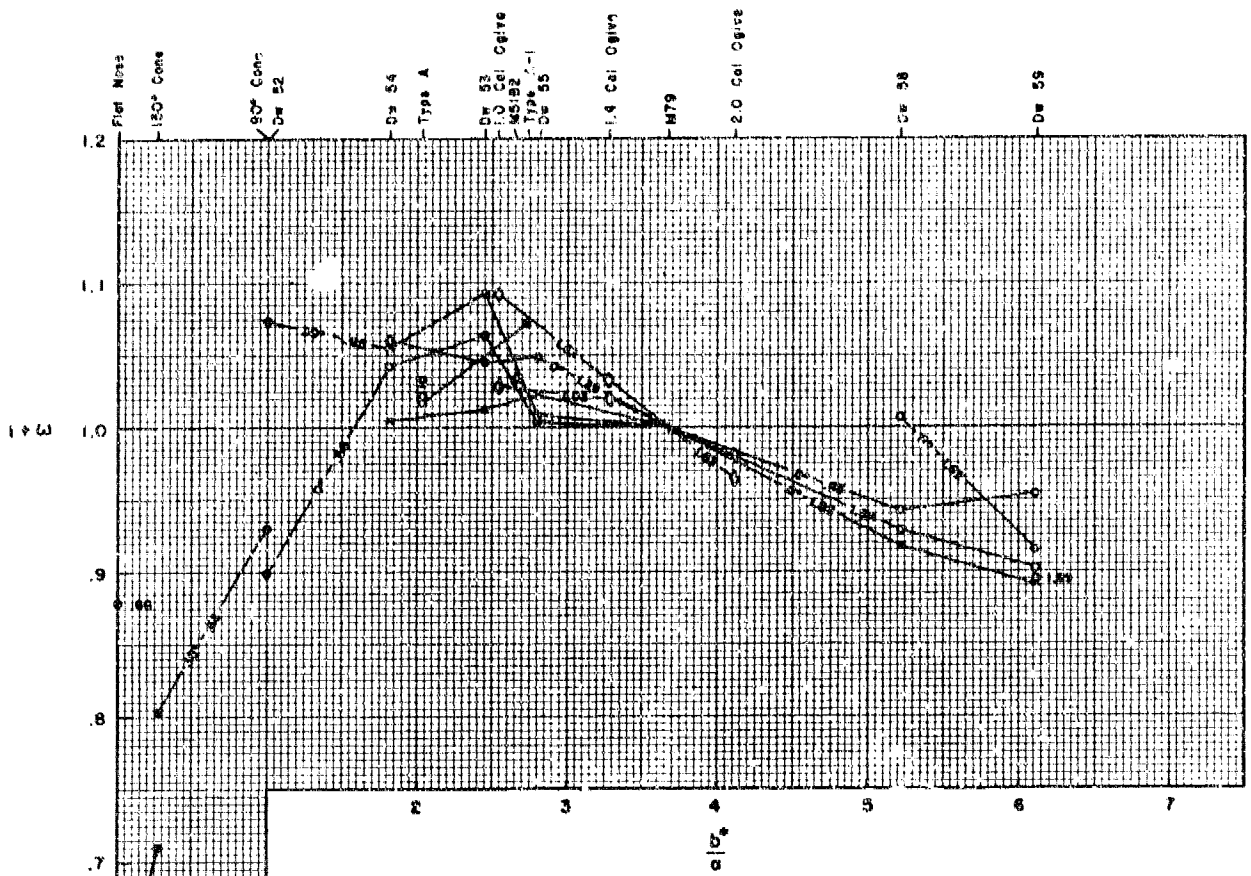

NPG PHOTO NO. 3047 (APL)

FIGURE (28)

THE OGIVE EFFECT

Monobloc Projectiles vs Homogeneous Plate at e/d > .5

- ○ 3" AP Monobloc Projectiles at 0° Obliquity
- ◉ " " " " " 30° "
- ◊ 2 pdr Projectiles at 0° Obliquity
- △ Uncapped 37mm AP Projectiles, average
- × Cal .60 AP Monobloc Projectiles at 0° Obliquity

e/d as indicated